EVALUATION OF EXTREME WIND AND WAVE CLIMATE AT KEAHOLE POINT, HAWAII

Richard E. Rocheleau

WORKING PAPER NO. 42

October 1979

SEA GRANT COLLEGE PROGRAM

University of Hawaii
Honolulu, Hawaii

EVALUATION OF EXTREME WIND AND WAVE CLIMATE AT KEAHOLE POINT, HAWAII

Richard E. Rocheleau

Report on the Sea Grant project, Extreme Wave Conditions for Selected Hawaiian Areas (R/EM-01); Charles L. Bretschneider, Principal Investigator; Sea Grant Years 08-09.

WORKING PAPER NO. 42

October 1979

SEA GRANT COLLEGE PROGRAM

University of Hawaii
Honolulu, Hawaii

This work reports on research funded in part by the University of Hawaii Sea Grant College Program under Institutional Grant Nos. 04-6-158-44026 and 04-6-158-44114 from NOAA Office of Sea Grant, Department of Commerce, and the Energy Research and Development Administration. The US Government is authorized to produce and distribute reprints for governmental purposes notwithstanding any copyright notations that may appear hereon.

ABSTRACT

The planning of any offshore or coastal facility depends strongly on the proper selection of the design wind and wave consistent with the climate at the chosen site. The extrapolation of available data beyond the record is critical for deepwater sites where depth limitations for approaching waves do not exist.

In this paper, the design wave for a deepwater site offshore from Keahole Point, 19°45' N latitude and 156°00' W longitude, has been obtained by extrapolating several sets of data using Gumbel's (1958) first asymptotic distribution. Comparison with several other extrapolation techniques shows this distribution to yield the smallest variance of the predicted to the hindcast or observed values for nearly all cases tested. The most probable design wave of a given return period is obtained in the following formula:

$$H = 14.21 + 4.78 \ln (T - .5)$$

where T = *the return period in years*

H = *the expected significant wave height in ft.*

Beyond the 19-year record of data used, 5.4 feed added to the expected wave height yields an 87 percent confidence of non-exceedance. This results in a 50-year significant design wave with an 87 percent confidence of non-exceedance of 38.3 (32.9 + 5.4) feet with a 12.5-second period for Keahole Point.

Run-up due to the 50-year significant wave and several smaller waves was predicted for several transects at Keahole Point. Even relatively large changes in the wave parameters resulted in small changes in the expected run-up. Run-up by the design wave was calculated as the greatest; that is, a run-up of 16.5 feet at a location 470 feet inland. At present it is possible only to approximate the run-up for this location. Detailed bathymetric data and wave measurement which would allow physical model testing should be carried out before specifically locating facilities at Keahole Point.

TABLE OF CONTENTS

LIST OF FIGURES

LIST OF FIGURES (continued)

Figure

Appendix B

LIST OF TABLES

Table

Appendix A

Appendix B

INTRODUCTION

The proper design of any deep ocean or coastal structure near Keahole Point on the leeward side of the island of Hawaii depends on an accurate prediction of the expected maximum wave conditions and the expected maximum wind velocities for the design life of the structure. Also important to proper coastal planning is an assessment of the inundation levels expected from the design storm.

Present approaches to determining design waves and winds often depend on the whims of the author to determine the distribution or plot to be used for analysis and the curve fitting technique to be employed. For this reason, the first part of this paper discusses the fundamentals behind the various methods and their applications. In Parts II and III these methods are used to analyze the available wave and wind data, respectively. The chosen design wave is based on the method which results in the best straight line fit. Although engineering judgment is necessary to choose suitable data, some of the arbitrariness of extrapolation is eliminated.

The result of this wave and wind analysis allows specification of the design storm for the area offshore from Keahole Point. The design waves for the western Hawaii region is useful for design projects or coastal planning including the inundation estimates presented in Part IV.

PART I. FUNDAMENTALS

Basic Probability and Data

The long-term prediction of expected wave heights and wind velocities depends on finding a suitable technique for extrapolating beyond the record of the tabulated data which are available. For any location there may be any number of sources of wave and wind data including weather station reports, shipboard observations, summary atlases, and hindcast results. Wave and wind observations from these sources are usually summarized in one of the following three ways:

1. By frequency of occurrence for the duration of the record
2. By partial duration series--the tabulation of all observed values above a chosen lower limit
3. By a maximum series--the largest value observed in each time interval

Several plotting techniques including several probability distributions have been used with each of the three data tabulations to allow extrapolation beyond the range of observation. These methods are each based on the assumption that if data fall on a smooth curve, the line may be extrapolated. For data available as a maximum series the more sophisticated asymptotic distributions have been used successfully.

Although details of application vary from method to method, each depends on defining a probability distribution function. Probability for these calculations is defined as the fraction of time during which a given event is expected to occur. The events are assigned a probability based on the relative frequency of occurrence observed in the data. A probability distribution function is defined by

$$F(X) = P(X \leq x) \tag{1}$$

where $F(X)$ is the probability distribution function and $P(X \leq x)$ is the probability that the outcome of a given trial will be less than or equal to x. This is also called the cumulative probability.

In engineering applications, it is useful to introduce the concept of return period (or recurrence interval). If $1/r$ is the fraction of trials for which $X > x_r$, then r is the return period in "trials" for the event x_r to be exceeded. The relation between the probability distribution function and return period is given as:

$$r = [P(X > x_r)]^{-1} = [1 - F(x_r)]^{-1}. \tag{2}$$

If a trial occurs every τ units of time, the return period in units of time will be

$$T_r = r\tau = \tau[1 - F(x_r)]^{-1} \tag{3}$$

where $F(x_r)$ is the value of the probability distribution function at x_r. Applying this to tabulations of wind and wave data the return period in years is

$$T_r = [1 - F(x_r)]^{-1}/n \tag{4}$$

where n = the number of observations per year.

For the special case where the data constitute a maximum series ($n = 1$), the return period is interpreted as the average duration in years between the events, x_r being the annual maxima.

Since the basis of each method is to provide a technique for extrapolating the probability distribution function beyond the range of observed data, $F(x)$ is always defined to be less than unity at the largest value of the variate. The region of cumulative probabilities between the largest calculated value and unity is associated with return periods longer than the record of data.

Plotting Methods

Except for data tabulated as a maximum series there is no widely applicable theoretical basis for determining the underlying probability distribution function or a suitable method of plotting the probabilities of exceedance calculated from the data. The condition generally used is that the data accurately fit by the chosen curve may be extrapolated. It is obviously best if the data are fit by a straight line. Several methods which have yielded such results in the past for wind and wave data and their application are discussed below.

Normal distribution

One of the simplest methods of analysis first used in hydraulic studies and later extended for design hurricanes and waves is Beard's (1952) method, which assumes a Gaussian distribution. In this analysis, the cumulative probability and recurrence interval are defined by

$$P(X \leq x_m) = F(x_m) = 1 - \frac{m + a}{M + b} \tag{5}$$

and

$$T_m = [1 - F(x_m)]^{-1}/n \tag{6}$$

where $F(x_m)$ = the assigned value of the probability distribution function of event m

m = rank of the observed value when ordered by increasing magnitude

M = total number of observed events

T_m = return period in years of event x_m

a, b = arbitrary constants to assure $0 < F(x) < 1$

n = number of observations per year.

The method associated with Beard is to plot $F(x_m)$ vs x_m on normal probability paper and then connect the points with a smooth curve which is extrapolated beyond the region of the observed data. For any return period of interest, the value of the probability distribution function is calculated and the expected value read from the plot. It is reasonable to assume that this simple procedure could be used in the long-term forecast of any parameter dependent on climatological phenomena.

Log-normal distribution

Following the work of Jasper (1956) and Darbyshire (1961), Draper (1963) has concluded that the height and period of the design wave can best be estimated from a Gaussian distribution of the logarithm of the height or period. This technique may be applied to whichever wave height parameter is required (i.e., mean wave height, significant wave height, etc.). The actual application of this technique for the determination of return periods beyond the record of the data is identical to Beard's (1952) method.

Weibull distribution

Weibull in 1951 proposed a simple distribution which has been used for various civil engineering problems. The application of this distribution to the description of wind wave short-term statistics was suggested by Bretschneider (1965). Several sets of wave data have been described by the Weibull distribution. For example, Battjes (1972), following some earlier work by Nordenstrom (1969), applied the Weibull distribution to 1 year of recorded data which was then linearly extrapolated to obtain the expected return periods. The Weibull distribution function is:

$$F(X) = 1 - \exp\left[-\left(\frac{x - A}{B}\right)^{C}\right] \tag{7}$$

where A = the lower limit of the variable x

B = the scale factor

C = the shape factor.

When the lower limit is zero (A Frechet distribution), as would be expected with wind and wave frequency data, rearranging equation (7) and taking the logarithm twice yields:

$$\ln \ln[1 - F(X)]^{-1} = C \ln x - C \ln B. \tag{8}$$

For data fit by this distribution, a plot of $\ln \ln[1 - F(X)]^{-1}$ vs $\ln X$ yields a straight line. The appropriate values of B and C are determined from the slope and intercept of the straight line.

Semi-log plot

Another technique which has been used by Mayencon (1969), Bretschneider (1973b), and many others involves plotting $\log [1 - F(X)]^{-1}$ vs x. If a linear relationship is obtained, extrapolation beyond the observed data should yield an acceptable estimate of the expected wave height or wind velocity for the design return period.

Discussion

The methods described above have been used by many authors for extrapolation of various wind and wave parameters. Due to the empirical nature of the use of these methods for extrapolation to long return periods, almost any data may be analyzed. However, there are several limitations.

Even with several possible distributions, it is rare that all the points will fall on a straight line. As described by Khanna and Andru (1974), the points at the extreme end often tend to curve off the line of best fit. Although tests are available for goodness of fit for the normal and log-normal distributions, they emphasize the dispersion around the central values but not for the extremes. Any plot allowing a linear reduction as in the Weibull distribution may be analyzed by least squares analysis weighting all points equally. However, to obtain a good fit at

the extremes, it may be necessary to arbitrarily weight the extreme data. This would be most evident in the analysis of frequency data where large amounts of data well below the maxima strongly influence the line of best fit.

If the data to be extrapolated constitute a maximum series, or are a summary of extreme conditions (as in hindcasts of the severest storms for a particular area), one or more of these methods with least squares analysis may yield accurate extrapolations. However, many authors have already concluded that when annual maxima are available, the better approach is Gumbel's (1958) extreme asymptotic distributions. Much of the remainder of this section describes asymptotic distributions and proposes a technique for application to a wider range of data.

Theory of Extremes--Asymptotic Distributions

A sophisticated approach to the determination of expected extreme values is based on the theory of largest values (Fisher and Tippet, 1928). When the underlying distribution of a variable is known, exact long-term models may be used. However, even in this case it is often easier to work with approximate models of the extreme trends. If the available data are the largest values (x_n) from many samples of $\underline{n}$ events each, the appropriate method is the asymptotic theory of extremes. Asymptotic theory is based on the stability postulate which states that the distribution of the largest value in Nn events will approach the same asymptotic expression as the distribution of the largest value in $\underline{N}$ samples of $\underline{n}$ events each. The asymptotic expressions are solutions of the equation

$$F^n(x) = F(a_n x + b_n) \tag{9}$$

where $F(X)$ = the underlying distribution function

a_n, b_n = constants based on sample size and the shape of the underlying distribution

n = number of events in each sample.

Since extreme values are relatively infrequent in occurrence compared with central values, the tail of the underlying distribution influences the distribution of extreme values more strongly than the central values.

The constraints of a_n and b_n and therefore the solutions of equation (9) are determined by the shape of the tail of the underlying distribution. Of concern in predicting the long-term maxima for wave and wind data are the constraints yielding the Fisher-Tippet Type I and Type III extreme value distributions. Type I model results as a solution of equation (9) with initial distributions unbounded in the direction of the extreme value, provided the tail decreases at least as rapidly as the exponential function (i.e., $F(x) = 1 - \exp[-a(x)]$ where $a(x)$ increase monotonically with x). The maximum series of the underlying normal, log-normal, and Weibull distributions are all modeled by the Type I distribution. The Type III model results from initial distributions which

are bounded in the direction of the extreme value. A complete derivation of the various extreme models is provided in Gumbel (1958).

The Type I model in the form of Gumbel's (1958) first asymptotic distribution (or double exponential distribution) has been used extensively to forecast the extreme values of certain environmental parameters. St. Denis (1975) has argued for the use of Gumbel's third asymptotic distribution (limited exponential asymptotic distribution) for the forecast of extreme wave parameters, based on the increased accuracy of a three-parameter system and the expectation that the distribution of sea states is bounded by physical considerations. However, due to the limited range of most observed data, and the relative ease of determining the parameters, the double exponential distribution has been used most often. The application of Gumbel's first and third asymptotic distributions is discussed below.

Gumbel's first asymptotic distribution

The first asymptote is described by the distribution function:

$$F(X) = \exp\{-\exp[-\alpha(x - \mu)]\} \tag{10}$$

where x = the variable interest

α, μ = parameters of the extreme distribution.

A linear reduction is made by introducing the reduced variate

$$y = \alpha(x - \mu). \tag{11}$$

Substitution of y into equation (10) yields

$$y = -\ln[-\ln F(x)]. \tag{12}$$

Gumbel has shown that the reduced variate (y) and return period (T) are related by

$$y = -\ln \ln T/(T - 1) \tag{13}$$

where T = the return period in the same time interval as the maximum series.

For large time interval T, this reduces to

$$y = \ln T - 1/2\ T \tag{14}$$

which has an error of only $\pm$ .7 percent for $T \geq 7$.

Solving equation (14) for T

$$T = \exp(y) + 1/2 \tag{15}$$

$$\simeq \exp(y) \text{ for large } T. \tag{16}$$

Substituting $y = \ln T$ into equation (11) yields $x = \ln/T\alpha + \mu$ which lends validity to the use of the semi-logarithmic plot for extreme data with an underlying exponential distribution for return periods greater than seven. Conversely, if the data were fit well by the logarithm of the return period vs x, it should be possible to use Gumbel's first asymptotic distribution for the analysis of these data.

Many techniques have been proposed for the proper selection of the parameters α and μ of the extreme distribution. These were often proposed for calculational convenience. With the proliferation of computers, one of the simplest methods is the use of least squares analysis. The line so determined represents the expected maxima at each return period. The actual values are dispersed around these expected values.

One significant advantage of the extreme value model is the applicability of confidence bands around the line of expected values. Two sets of confidence bands may be calculated. The first is a function of the reduced variate and slope and is used to determine the goodness of fit of the assumed distribution. The second is a function of the slope only and is used to predict confidence levels of the extreme values. The step by step procedure for applying Gumbel's first asymptotic distribution and the calculation of the confidence bands are outlined in Appendix A.

Gumbel's third asymptotic distribution

This is described by the probability distribution function

$$F(X) = \exp - \left(\frac{x - \mu}{\hat{x} - \mu} \right)^k \tag{17}$$

where μ, $\hat{x}$, and k are parameters of the extreme distribution such that

μ = the modal value

$\hat{x}$ = the asymptotic limit

k = the shape factor.

A reduced variate defined by $y = -\ln [-\ln F(X)]$ yields the relationship

$$y = -k \ln \left(\frac{x - \mu}{\hat{x} - \mu} \right) \tag{18}$$

so that

$$x = \mu + (\hat{x} - \mu) \exp(-y/k). \tag{19}$$

The return period T is again approximated by

$$T \simeq \exp(y) + 1/2. \tag{20}$$

Evaluation of the three-parameter system is difficult. Normal regression techniques are also difficult to apply and expensive to use due to the shape of the function. A program of trial and error described in

Appendix A provides a method of solving the equation for any desired variance. Confidence bands have not been as thoroughly analyzed as for the first asymptotic distribution. However, St. Denis (1974) stated that a similar method as in Gumbel's first asymptotic distribution with varying slope is applicable. A summary of this calculation is also presented in Appendix A.

Analysis of Frequency Data by Extreme Value Distributions

Applications of extreme value asymptotic distributions are severely restricted by the scarcity of data tabulated as a maximum series. Quite often for waves and not infrequently for winds, data are available only as a summary of the frequency of occurrence or as a tabulation of all reported values for several years. Yearly maxima are not readily available from this type of summary. In the past, these data were analyzed by one of the methods described previously, sometimes with an arbitrary weighting of the larger values. The following discussion describes a procedure to estimate the expected yearly maxima from the tabulated frequencies so that Gumbel's distributions may be used.

Since the extreme value distributions require an input of discrete points, the frequency distribution is interpolated linearly to generate the same number of discrete data as reported observations. A suitable approach for those cases where the number of observations is not available is to assume one datum point per .1 percent of the observations. The user must be sure that these tabulations do not exclude the very infrequent maximum values.

If the cumulative probability of a single independent event being less than or equal to x_m is given as

$$F(x_m) = P(X \leq x_m), \tag{21}$$

then the probability of n independent trials all being less than or equal to x_m is

$$P'(X \leq x_m) = [F(x_m)]^n. \tag{22}$$

If n is the number of independent observations in a year, then $P'(X \leq x_m)$ is the expectancy of an event of magnitude x_m being the annual maximum. The return period, Ty, in years is then found to be

$$Ty = [1 - P'(X \leq x_m)]^{-1} = \{1 - [F(x_m)]^n\}^{-1} \tag{23}$$

This return period is longer than that calculated as

$$T_m = \frac{[1 - F(x_m)]^{-1}}{n} \tag{24}$$

since the former does not consider events occurring in the same year as a larger magnitude event. Langbein (1949) has shown that as the recurrence interval increases, the two values approach each other. Figure 1, after

Langbein, shows the relationship between the two return periods. For return periods greater than 10 years, the difference is negligible.

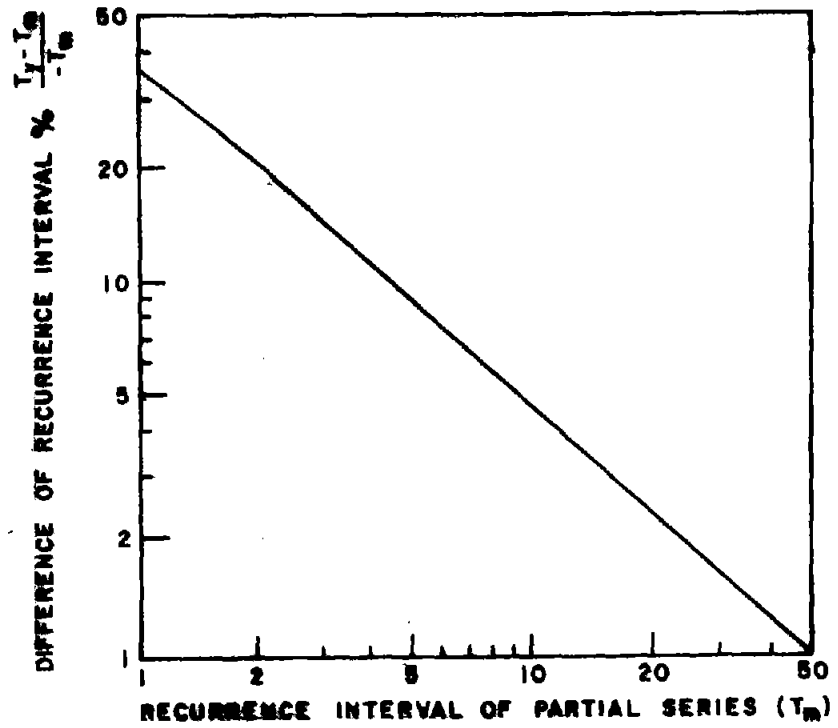

Figure 1. Comparison of recurrence interval from a maximum series and a partial duration series (After Lanbgein, 1949)

One limitation of this technique is the need to assume the independence of the observations. It may be possible that a severe storm of long duration in the area of interest contributed to several of the larger values. Unfortunately, there is usually no way to ascertain dependence or independence. Whatever the relation between the variables, analysis by this technique often yields a linear relation when using Gumbel's double exponential distribution.

In application, the frequency data are terminated at a value equivalent to the smallest annual maxima expected in order to create a partial duration series. In hydraulic applications, partial duration series are normally chosen to represent an average of one to four events per year. This seems to be a reasonable approach for wave and wind data also.

Design Life and Risk Factors

In the design of an ocean structure the engineer needs to determine the risks involved in selecting the design wave. The calculated return period is the average expected duration between events of a given magnitude; however, this value provides no indication as to when the event may occur. Court (1952) and others have related design life, design return period, and risk in simple probabilistic terms to aid the design engineer. The argument presented is summarized here.

Assuming the annual maxima to be independent, the probability that x_m will not be exceeded in $\underline{N}$ years is given by

$$[P'(x \leq x_m)]^N. \tag{25}$$

The probability of at least one more exceedance in $\underline{N}$ years is

$$P(X_{max} > x_m) = 1 - [P'(X \leq x_m)]^N. \tag{26}$$

Substituting T_y from equation (23) yields

$$P(X_{max} > x_m) = 1 - (1 - 1/T_y)^N. \tag{27}$$

$\underline{N}$ may be considered as the design life with a probability of failure given by $P(X_{max} > x_m)$ for the event with a return period T_y. For convenience the design life is defined in terms of return period by

$$N = T_y/U \tag{28}$$

where U is a positive value ≥ 1.

For design calculations, the value $P(X_{max} > x_m)$ is considered as the risk (R) factor. Substituting R into equation (27) yields

$$R = 1 - (1 - 1/T_y)^{T_y/U}. \tag{29}$$

For large T_y this becomes

$$R = 1 - e^{-1/U}. \tag{30}$$

Solving for the factor U in equation (30),

$$U = -1/\ln(1 - R). \tag{31}$$

Substituting equation (31) into equation (28) yields

$$N = -T_y[\ln(1 - R)]. \tag{32}$$

Thus, for a chosen design life and risk factor, the necessary design return period may be calculated.

Adjustment of Data to Obtain Set Maxima

The values determined from any of the techniques discussed do not necessarily represent the absolute maximum expected. Due to the irregularity of the seaway, the maximum wave height in a given sea state may vary substantially from the observed or significant wave height. Likewise, there may be a correction to the wind velocity due to the disparity between the sampling duration and the sampling interval, as well as differences between mean and peak values.

Waves

The irregularity of the sea is modeled using a frequency or period spectrum. From the assumed spectral width and characteristic wave period it is possible to relate various characteristic wave heights. For this purpose the significant wave heights are generally assumed to be Rayleigh distributed, although for severe sea states this may not be an accurate characterization.

The expected average value of the highest 1/n waves in a Rayleigh distributed sea state is given as

$$E\left[\overline{\xi}_1/n\right] = \int_0^\infty \left\{ 1 - \left[1 - e^{-\left(\frac{x^2}{2m_o}\right)} \right]^N \right\} dx \tag{33}$$

$$E\left[\overline{\xi}_1/n\right] = n\sqrt{2m_o} \left\{ \left[\frac{1}{n} (\ln n)^{1/2}\right] + \sqrt{\pi}\,[0.5 + \operatorname{erf}(2 \ln n)] \right\}^{1/2} \tag{34}$$

where ξ = the wave amplitude

m_o = the mean square value of the wave elevation at the point under consideration

An asymptotic expression for the maximum expected wave in a given sea state is

$$E\left[\xi_{max}\right] = \sqrt{2m_o} \left[(\ln n)^{\frac{1}{2}} + 0.2886 (\ln n)^{-\frac{1}{2}} \right] \tag{35}$$

The ratio of the expected maximum wave height to the significant wave height $(\overline{\xi}_{1/3})$ yields an aggradation factor

$$H_{max} = f_r = \frac{(E\ \xi_{max})}{(E\ \overline{\xi}_{1/3})} = \sqrt{\frac{1}{2} \ln n} \tag{36}$$

The expected number of waves, n, is calculated from the ratio of the time interval of interest and the mean wave period. Many authors have concluded that for practical applications this value should not exceed 1.8.

Winds

The great variability of wind with time and location leads to many difficulties in making forecasts of extreme conditions. Unfortunately, few weather stations record data with sufficient accuracy to allow the relationships among mean wind speed, peak wind speed, and instantaneous gust speed to be determined for that specific location. In practice, if all types of wind data are not available, one can use gust factors relating the various measures of wind velocity. The *Handbook of Geophysics* (US Air Force, 1961) contains several tables of such values including the typical wind variations specific to hurricane wind fields. Table 1 shows probable gust factors for a variety of mean hourly wind speeds and varying gust lengths. In general, larger gust factors will occur for the shorter duration of the peak wind speed and for longer time intervals of the mean wind speed.

TABLE 1. OVERWATER WIND AND WIND FORCES

Mean Hourly Wind Speed (knots)	Period t (sec)						
	600	60	30	20	10	5	0.5
20	1.10	1.25	1.30	1.35	1.40	1.50	
30	1.10	1.23	1.33	1.37	1.43	1.47	
40	1.10	1.25	1.32	1.35	1.42	1.48	(1.63)
50	1.08	1.24	1.32	1.36	1.42	1.48	(1.64)
60	1.08	1.23	1.31	1.35	1.42	1.48	(1.60)
70	1.08	1.24	1.31	1.35	1.42	1.49	(1.59)
80	1.09	1.24	1.33	1.36	1.43	1.48	
Average	1.09	1.24	1.32	1.36	1.42	1.48	(1.61)
G/U* (10 min)	1.00	1.15	1.21	1.25	1.30	1.36	1.48
G/U (1 min)	--	1.00	1.07	1.10	1.15	1.19	1.30

Source: Values calculated from data presented in Whittingham, 1964

Note: Probable values of the maximum gust factors averaged over short periods of time t when mean hourly wind speed has various values

*G/U = gust speed/wind speed

PART II. WAVES

A statistical analysis of the wave climate for any location is a very complex problem. Observed gravity waves may be due to generation by local winds or they may have been generated by distant storms having propagated to the area of interest. Wind waves or seas are generally short-crested, irregular waves with variable direction of propagation. Swells from distant generation areas are characterized by longer wave periods, less temporal variation in the wave frequency, and generally a more uniform direction of propagation. At any instant, however, the seaway may be composed of the superposition of irregular wind waves and swell.

The most frequently used representation of a complex seaway makes use of a directional variance spectrum to describe the energy contributions due to a particular frequency band and direction of propagation. The spectrum may be easily calculated from detailed wave recordings. Such a spectrum combines the contributions from all directions for the average seaway in Hawaiian waters as calculated by St. Denis (1974) is presented in Figure 2. In this hypothetical seaway, the contributions due to the

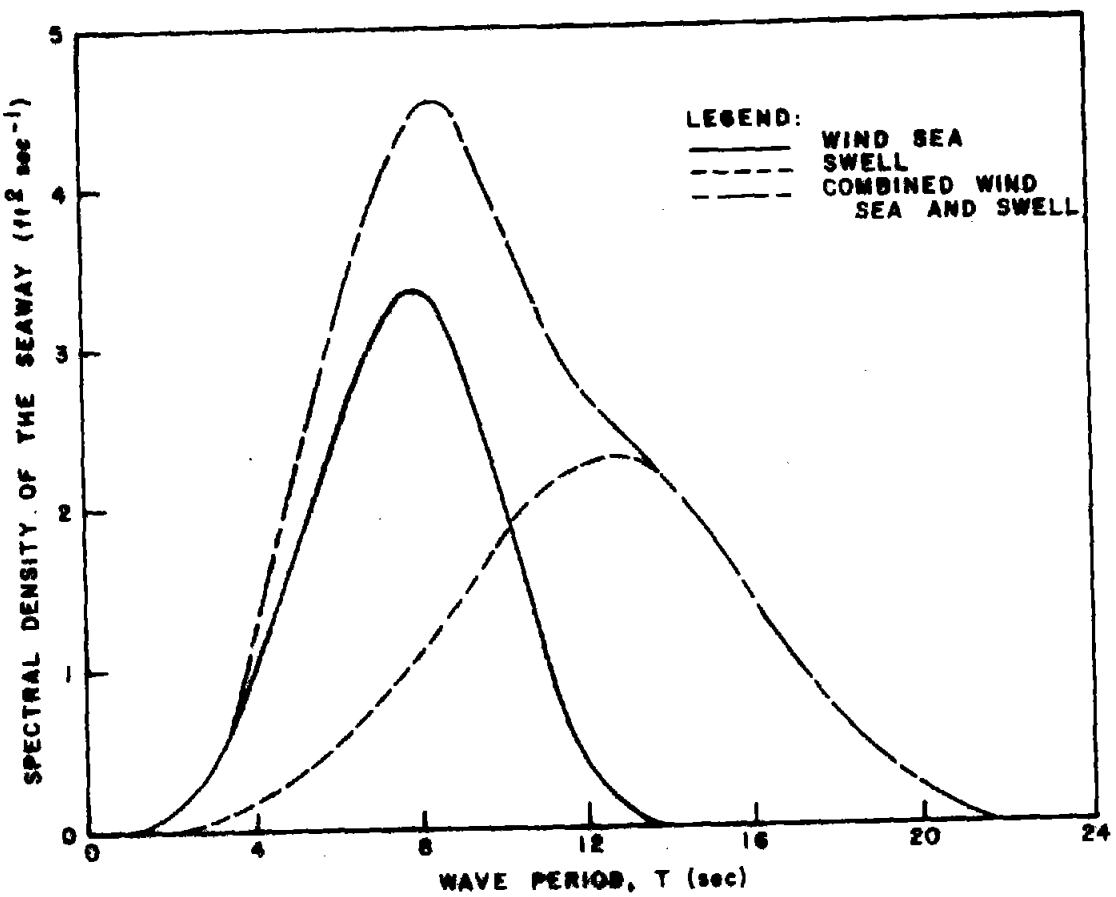

Figure 2. Energy spectrum of the average seaway in Hawaiian waters (After St. Denis, 1974)

wind sea and swell are shown separately. The information available from spectral records includes the expected significant and maximum wave heights and mean wave periods for the sea state modeled.

For design purposes it would be ideal to have a continuous summary of the parameter of interest for many years. From the expected extreme wave height calculated from such a record, a possible short-term spectral description of the seaway could be synthesized to yield other parameters. Unfortunately, the short-term description of severe sea states has not been well defined except for specific situations such as for seas generated by a hurricane.

Wave Climate in Hawaiian Waters

Waves affecting waters around the Hawaiian islands result from storms in all parts of the Pacific Basin and even in parts of the Indian Ocean. The superposition of distant and locally generated waves together with the influence of the islands result in a complex wave climate which shows considerable spatial variability. The wave climate for the islands has been classified into four general types characterized by wave height, wave period, and direction of approach. Figure 3, adapted from Inman, Gayman and Cox (1963) and Moberly and Chamberlain (1964), shows the direction of approach of the four main wave types. A short description of each follows.

1. Northeast tradewind waves. Northeast tradewind waves are present a large percentage of the time, but dominate from April to November when the tradewinds are present 90 to 95 percent of the time. The tradewinds blow 12 to 15 knots per hour about 50 percent of the time generating waves from 4 to 11 feet in height with periods of 5 to 9 seconds due to the long uninterrupted fetches. These waves approach the island from the north to the southeast.

2. Southern swell. Southern swell approaches from between the southeast and the southwest. It is most frequent from April through October, resulting from severe winter storms in the southern hemisphere. Due to the decay over the distances, these waves usually arrive as low, long-period swell, typically 1 to 6 feet high with periods of 14 to 22 seconds. However, swell substantially larger than 6 feet has been observed along the southern boundary of the islands.

3. Kona storm waves. These waves approach the islands infrequently with the passage of kona storms which are generally cold-core, low-pressure systems of large radius. During the passage of such systems the tradewinds are replaced by south or southwesterly winds generating waves which arrive from the southeast to west. Although infrequent, the severity of kona storms varies from a light breeze to gale strength. The associated wave climate varies over a wide range. Waves of 10 to 15 feet with periods of 8 to 10 seconds are not uncommon.

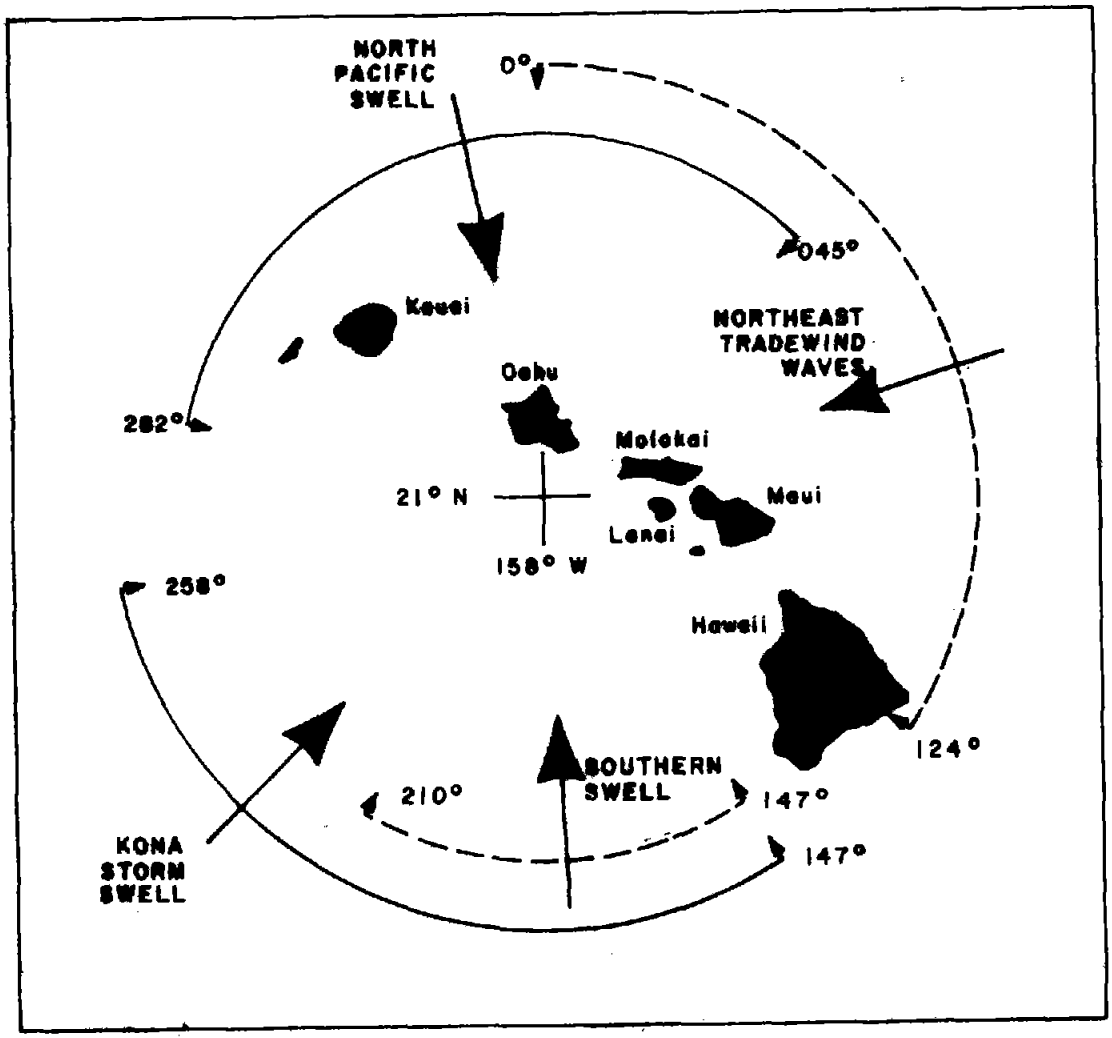

Figure 3. Approach directions of frequently occurring waves in Hawaiian waters (After Moberly and Chamberlain, 1964)

4. North Pacific swell. North Pacific swells, having been generated by severe storms near the Western Aleutians or from mid-latitude low pressure systems, approach the islands from the north. These waves are most frequent from October through May and are responsible for the large surf observed in many areas.

Since the different types of waves are due to generation in different areas, several may occur simultaneously. The reported frequencies of occurrence for these wave types are based on the summary of the Marine Advisers' (1964) report which classifies waves by frequencies of occurrence according to the following parameters:

1. Wave direction: sixteen sectors of 22.5° each

2. Significant wave height: 2-ft intervals up to 19 ft; one category over 19 ft

3. Significant wave period: 2-sec increments from 3 to 19 sec; one increment over 19 sec

The results are based mainly on data obtained from wave recorders in operation at Kahuku Point and Barbers Point, Oahu from July 1962 through June 1963. However, data for winter months, especially for kona conditions, are based on hindcasts from weather charts for judiciously chosen months. Although intended for specific use around Oahu the results are considered representative of the general conditions for all the Hawaiian islands and are frequently used to represent the "typical" wave climate from the direction of interest.

Although not included in many discussions of Hawaiian waves, a fifth type of wave is important for design considerations. Large waves produced by passing hurricanes may affect many island locations. These tropical cyclones are characterized by a warm low-pressure core with sustained wind speeds substantially higher than those associated with tropical (kona) storms. For many locations the expected extreme waves will be due to the passage of such storms. Figures 4 and 5 show the paths of several severe storms and hurricanes which have affected the islands.

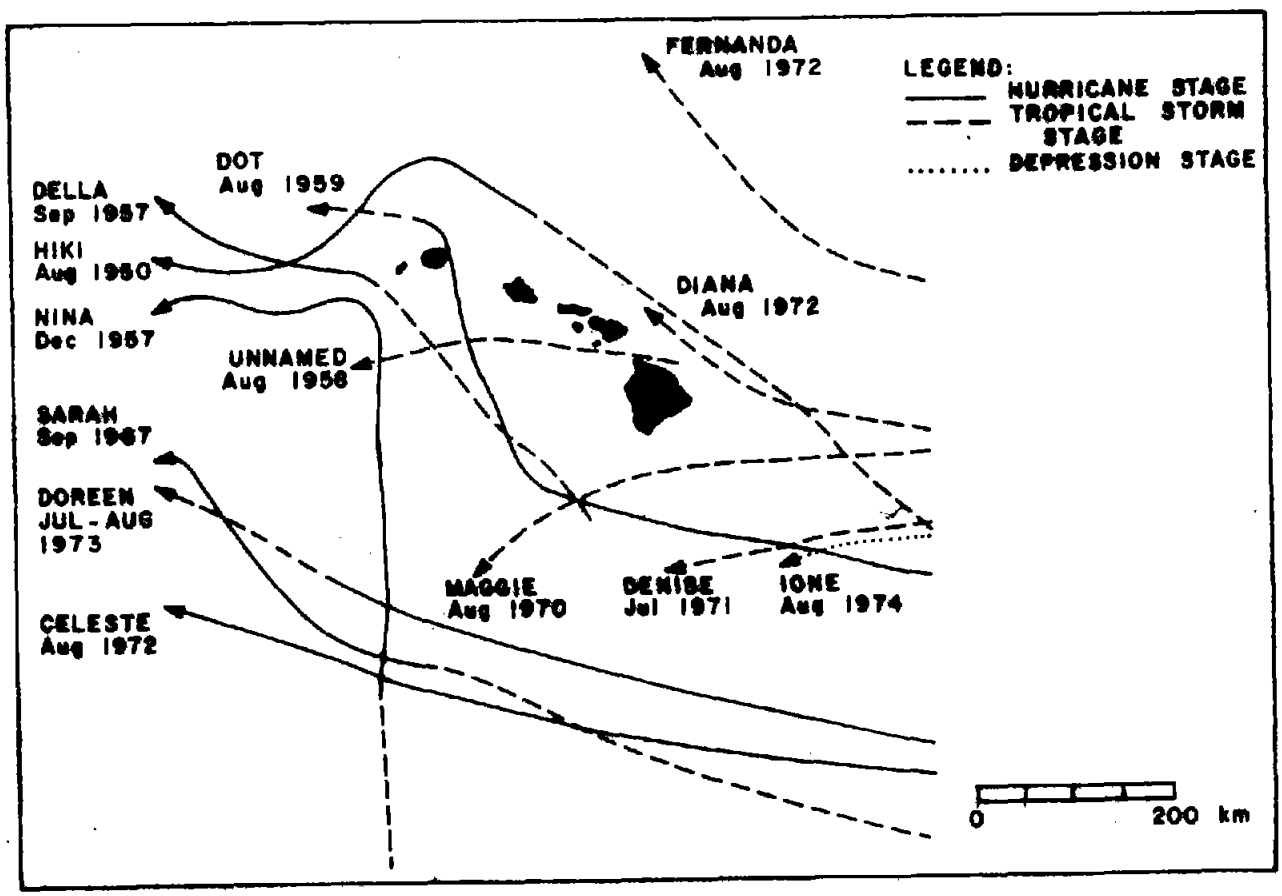

Figure 4. Tracks of hurricanes and tropical storms in the vicinity of the Hawaiian Islands for the period 1950-74 (Figure provided by the National Weather Service of the National Oceanic and Atmospheric Administration of the US Government)

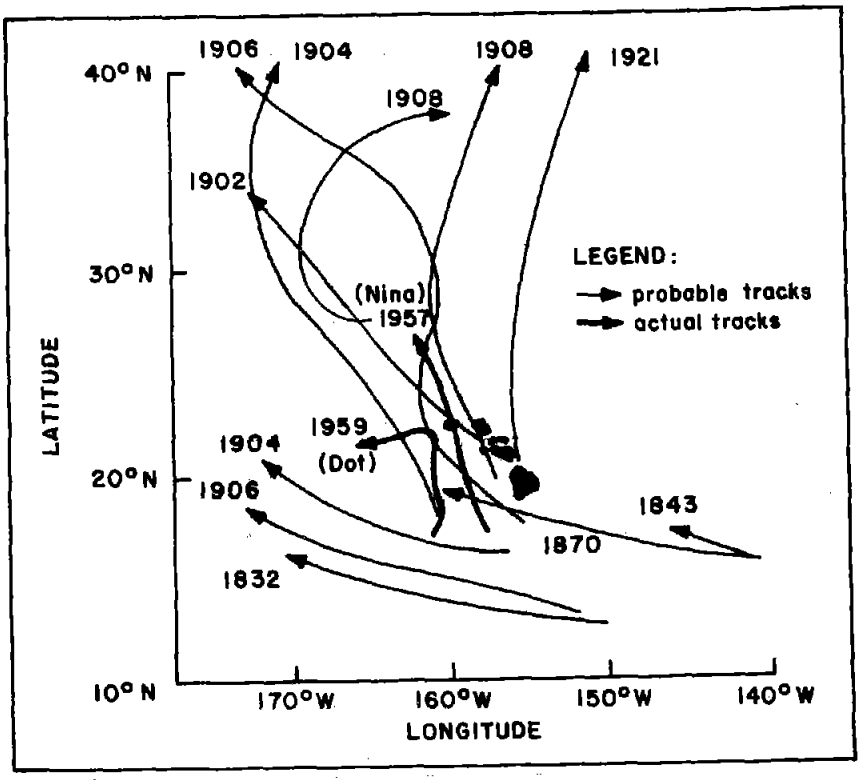

Figure 5. Historical tropical cyclone tracks near the Hawaiian Islands (After St. Denis, 1974)

Design Wave Data for Keahole Point

The wave climate at Keahole Point is strongly influenced by the sheltering effect of Hawaii and the other islands. Except for a small window between 003°T and 016°T, the waves approach the point from between the south-southeast and the west-northwest. Figure 6 shows these approach directions. In the past, large waves affecting Honokohau Bay not far from Keahole Point have been generated by storms in the sector from 168°T to 310°T. Large waves generated by frequent winter storms north of the islands may pass through the Alenuihaha Channel and should be considered.

The accurate prediction of expected extreme wave heights at Keahole Point is made difficult by the absence of a continuous wave record for the area. Predictions must therefore be based on shipboard observations and hindcasts of severe storms. The procedures described in Part I have been applied to determine the best method of extrapolation, the line of best fit, and, where possible, the reliability of the results. Three sources of data have been analyzed to determine long-term wave heights. These are described below.

1. Marine Advisers: *Severe Storm Wave Characteristics in the Hawaiian Islands* (1963)

This report presents the results of a hindcasting program to determine the wave conditions produced by the 10 most severe storms of the 15-year period from 1947 through 1961 for all Hawaiian waters.

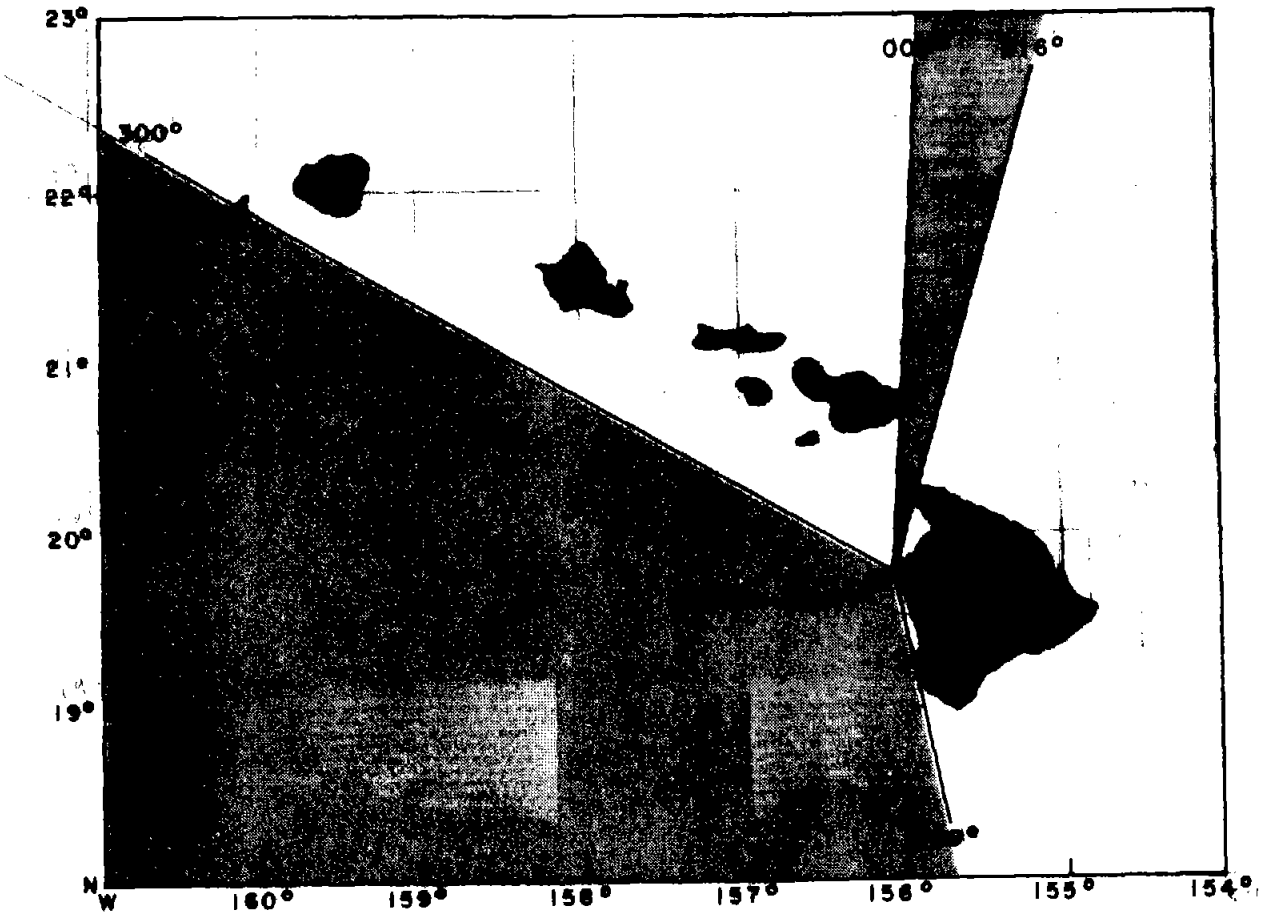

Figure 6. Generation areas from which waves may approach Keahole Point

These hindcasts were specific for waves approaching either the west coast of Lanai or the west coast of Molokai. Certainly not all the storms analyzed would have affected Keahole Point and even those which did may have had considerably altered wave characteristics at that location. However, these 10 most severe storms, without regard to sheltering effects or direction, were analyzed to provide an upper limit on the severity of the deepwater wave climate expected to occur. The results of the hindcasts for the 10 storms are shown in Table 2. The direction of wave approach to the islands is shown in Figure 7. A complete discussion of the storm systems involved may be found in the Marine Advisers' (1963) report.

2. Corps of Engineers: Hindcasts for Harbor Planning

The US Army Corps of Engineers, Honolulu District recorded hindcasts of 17 storms affecting the Hawaiian Islands from 1947 through 1965. Seven of these which resulted in severe waves at Honokohau Bay are applicable to Keahole Point. In addition, four storms north of the islands which generated large swell from a direction possibly affecting Keahole Point have been included. The inclusion of these storms is based on the location of the generation area relative to the window between Maui and Hawaii rather than on actual observations.

TABLE 2. HINDCAST WAVE CHARACTERISTICS FOR 10 STORMS FROM 1947 THROUGH 1961

Storm Date	Significant Wave Height (ft)	Significant Wave Period (sec)	Direction (°True)
Jan 3, 1947	15.7	16.4	0
Mar 6, 1954	25.0	17.2	027
Nov 27, 1956	12.8	16.8	332
Dec 2, 1957	32.5	14.5	185
Jan 12, 1958	27.1	23.5	310
Nov 22, 1958	12.5	14.6	0
Jan 18, 1959	7.0	13.5	268
Aug 6, 1959	16.8	15.9	148
Dec 11, 1960	18.0	19.6	315
Dec 20, 1960	13.8	18.0	332

Source: Marine Advisers, 1963

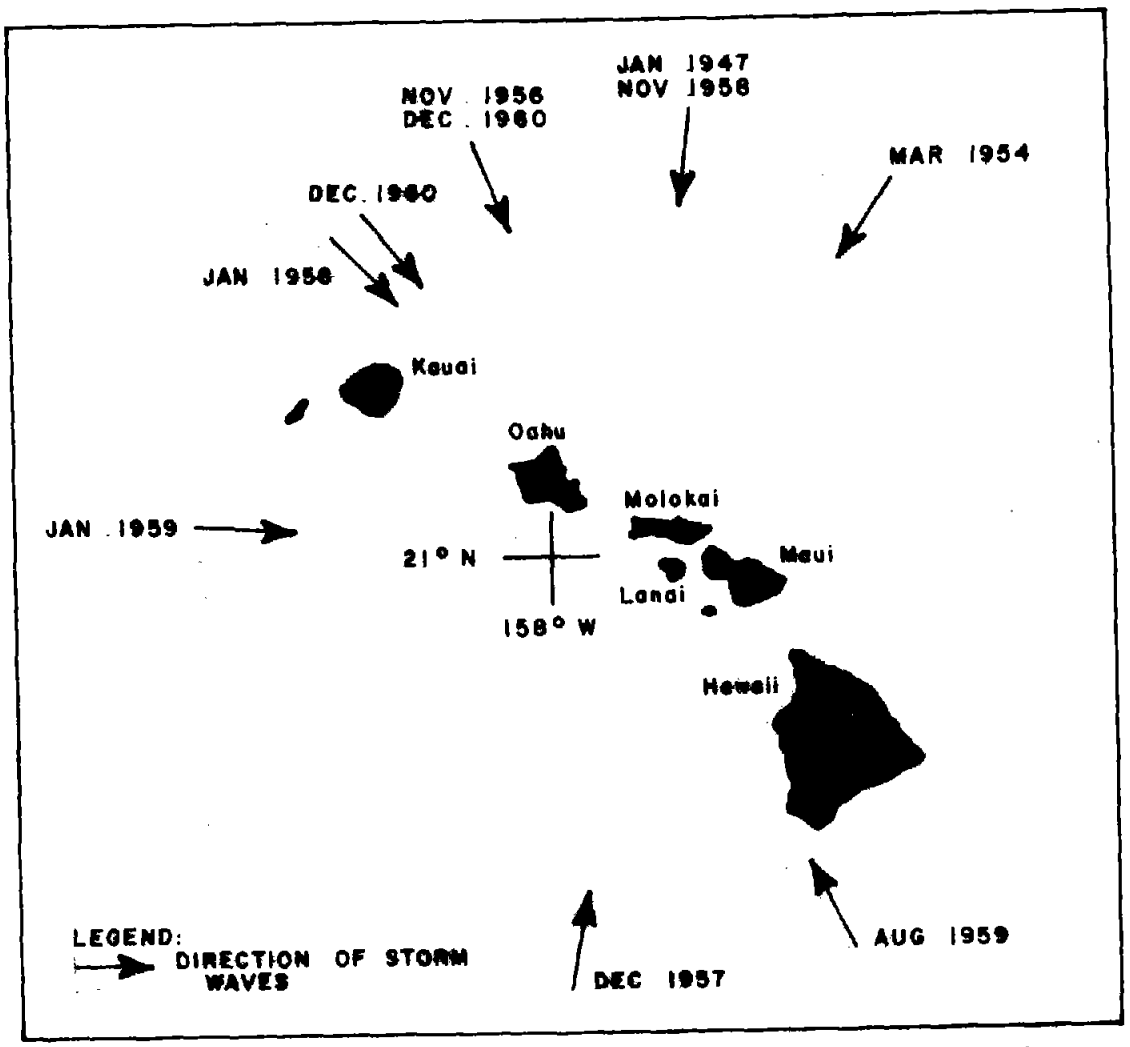

Figure 7. Direction of wave approach to the Hawaiian Islands from 10 storms hindcast by Marine Advisers from 1947 through 1961 (After Marine Advisers, 1963)

Table 3 summarizes the hindcast results specific to Keahole Point. The approach directions of the waves from the 11 storms are presented in Figure 8.

3. US Navy Hydrographic Office: *Summary of Synoptic Meteorological Observations* (SSMO)

The *Summary of Synoptic Meteorological Observations* provides a monthly and annual summary of over 16,000 individual shipboard wave observations over the 8-year period from 1963 to 1971. The waves are classified by observed (assumed to be significant) wave height and by observed wave period, but not by direction. The observations are summarized in Table 4. Although the direction of wave approach is normally essential to determine the affected locations, based on Figure 9 which shows the boundaries of SSMO Area 2, it has been assumed that any sea state observed in the area could have affected Keahole Point. Similarly, all waves which affect the point would propagate through the observation area. Unfortunately, there are no data which actually show the observations in SSMO Area 2 to be representative of Keahole Point.

Both the shipboard observations and hindcast results may be in error because they are not instrument-measured values. Hindcasts for the first two sources of data were made using the Sverdrup-Munk-Bretschneider method. The outputs reported are the significant wave height and period. The necessary inputs including fetches, duration, and wind speeds were obtained from synoptic weather charts.

Marine Advisers (1964) reported two sources of possible error in hindcasting. The first deals with the substantial opportunity for human or mechanical error in obtaining and transcribing data. Over the oceans where data are relatively sparse, improperly entered data may have been difficult to detect and eliminate from the meteorological record. The second problem in hindcasting concerns the subjectivity of determining the meteorological parameters. This again is especially true in regions of sparse data; for instance, sparse data make accurate determination of isobaric spacing difficult. Marine Advisers stated, "The configuration the forecaster draws then becomes in large measure a reflection of his own judgement and past experience."

SSMO tabulations were scrutinized to eliminate obvious errors. Unfortunately, there is no rigorous technique to decide on the inclusion or exclusion of questionable values. One feature which must be considered is the difference between instrumentally measured significant wave heights and visually observed heights as presented in the SSMO tables. No correlation between these values is included in the SSMO publication, but several such correlations have been determined and have been summarized by St. Denis (1975) and are included in Table 5.

As shown in Table 5 the observed wave heights may be larger or smaller than the corresponding instrumentally measured significant wave heights. Within the range of design wave heights calculated in the next section, comparison with one of the most widely accepted correlations--the Hogben and Lumb fit--shows the observed values to be approximately .5-meter smaller

TABLE 3. HINDCAST WAVE CHARACTERISTICS FOR 11 STORMS AFFECTING KEAHOLE POINT FROM 1947 THROUGH 1965

Storm Date	Significant Wave Height (ft)	Significant Wave Period (sec)	Direction (°True)
Jan 3, 1947	14.5	17.3	005
Mar 6, 1954	22.9	17.2	020
Dec 20, 1955	14.8	11.2	270
Sep 5, 1957	18.9	21.1	286
Dec 2, 1957	25.5	13.4	210
Nov 22, 1958	14.6	14.3	357
Jan 18, 1959	14.0	9.6	267
Aug 6, 1959	22.5	12.0	255
Jan 7, 1962	13.6	11.1	222
Jan 16, 1963	23.0	14.5	300
Feb 2, 1965	27.0	17.2	010

Hindcasts from the US Army Corps of Engineers, Honolulu District, 1968

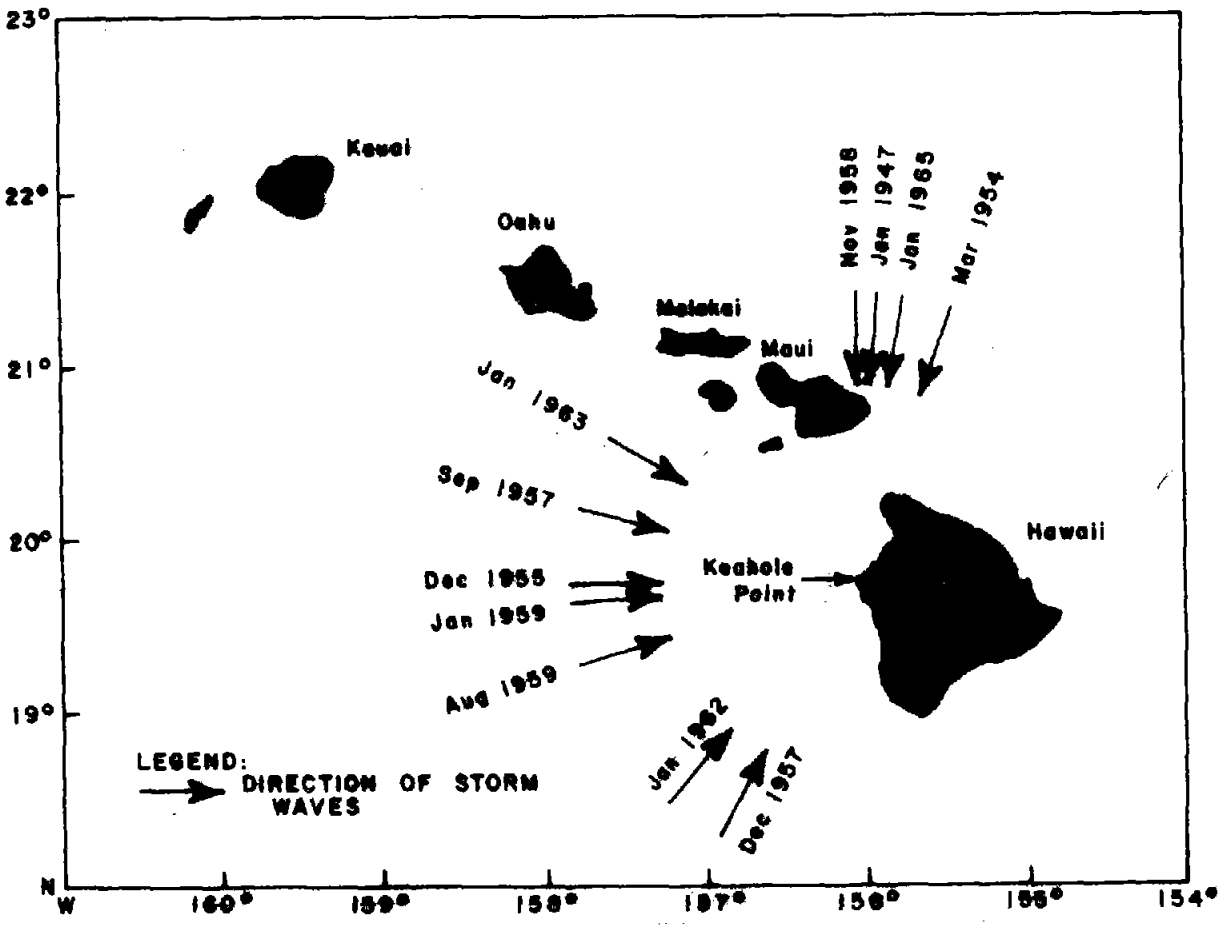

Figure 8. Direction of wave approach to Keahole Point from 11 storms hindcast by the Corps of Engineers from 1947 through 1965 (After US Army Corps of Engineers, Honolulu District, 1968)

TABLE 4. SUMMARY OF 8 YEARS OF SHIPBOARD OBSERVATIONS LEEWARD OF THE HAWAIIAN ISLANDS TABULATED AS PERCENTAGE OF FREQUENCY OF OCCURRENCE

Period (sec)	Wave Height (ft)													Total
	1	1-2	3-4	5-6	7	8-9	10-11	12	13-16	17-19	20-22	23-25	26-32	
6	1.5	12.5	21.2	8.3	3.2	1.0	.3	.1	.1	.0	.0	.0	.0	7,978
6-7	.1	2.1	8.1	8.6	6.2	2.2	.9	.3	.2	--	--	--	.0	4,707
8-9	--	.4	2.2	2.8	2.8	1.6	1.0	.4	.2	--	--	--	.0	1,884
10-11	.0	.1	.5	.7	.7	.6	.4	.2	.2	--	--	--	.0	548
12-13	.0	--	--	.2	.3	.2	.1	--	.1	.0	.0	--	--	163
13	.0	.0	.0	.1	.1	.1	--	--	--	--	--	.0	.0	64
Indet	3.6	1.1	1.1	.6	.2	.1	.1	--	--	.0	.0	.0	.0	1,102
Total	852	2,696	5,501	3,476	2,218	956	455	152	106	14	9	10	1	16,446
Percentage	5.3	16.2	33.1	21.2	13.6	5.9	2.8	.9	.7	.1	.1	.1	--	100.0

Source: US Navy Weather Services, *Summary of Synoptic Meteorological Observations*, Area 2

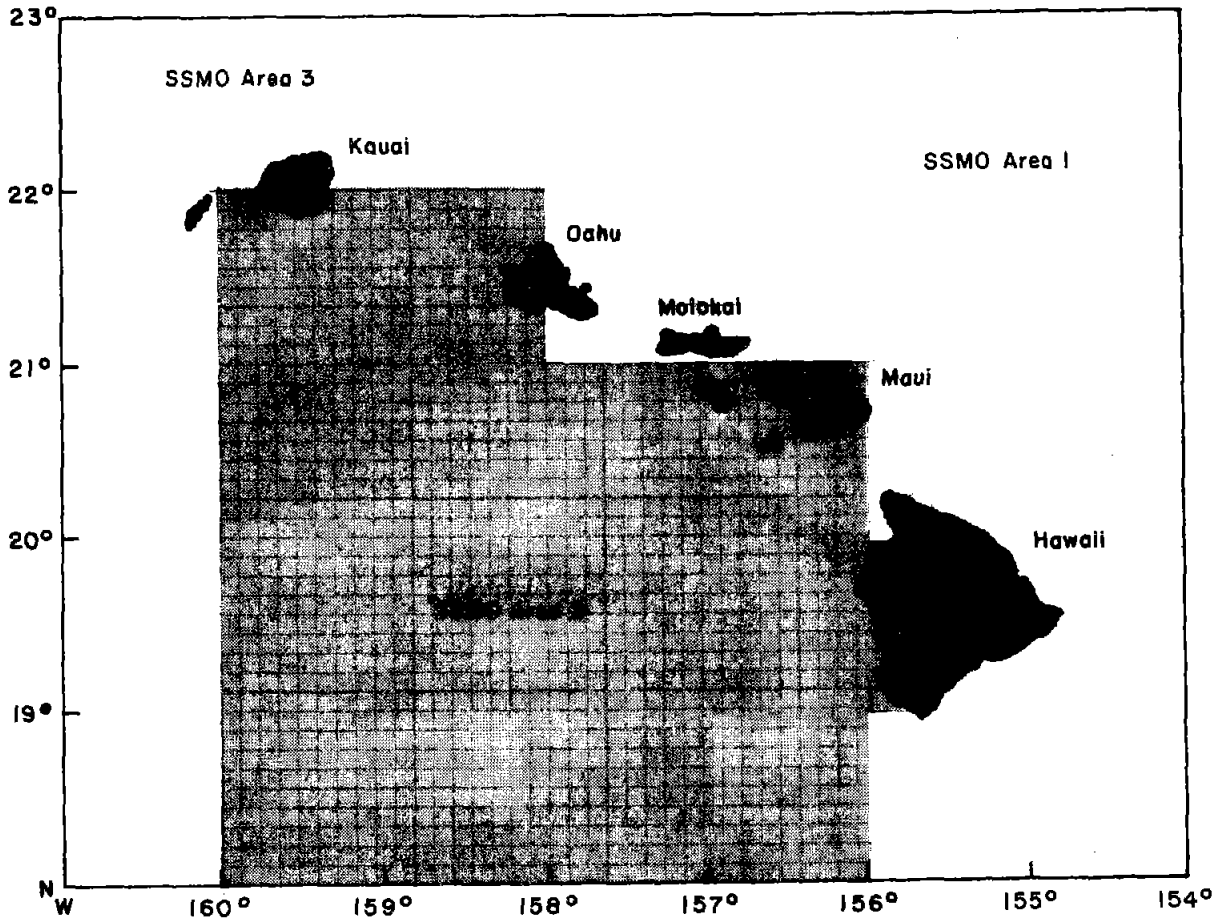

Figure 9. Boundaries of the SSMO Area 2

TABLE 5. CORRELATION BETWEEN INSTRUMENTALLY MEASURED AND OBSERVED WAVE HEIGHTS

Reference	Wave Heights (m)
Brooks and Jasper, 1957	$H_s = 1.088\ H_{obs}$
Cartwright, 1964	$H_s = 1.17\ H_{obs}$
(stations I and J)	$H_s = 1.28 + .88\ H_{obs}$
Nordenstrom, 1969 (fit to Cartwright data)	$H_s = 1.78\ H_{obs}^{0.72}$
Hogben and Lumb, 1967	$H_s = 1.05\ H_{obs}$
(stations A, I, J, and K)	$H_s = 1.23 + .89\ H_{obs}$
Nordenstrom, 1969 (fit to Hogben and Lumb data)	$H_s = 1.51 + .848\ H_{obs}$

Source: St. Denis, 1974

than the calculated significant value. In the remainder of this report, the observed heights tabulated in SSMO tables are discussed as significant wave heights.

It must also be realized that SSMO data are based on shipboard observations and that vessels avoid severe seas when possible. This may cause a bias toward design wave heights lower than actually present.

Analysis and Results

The data from the hindcasts were analyzed by the five methods described in Part I. The lines of fit for the normal and log-normal distributions were calculated from the mean and standard deviation of the reported wave heights. The lines of best fit for the Weibull and the asymptotic distributions and the semi-log plot were determined by least squares. Confidence bands were calculated for Gumbel's first asymptotic distribution to test the validity of the line and to yield confidence levels for values beyond the duration of the record. Details of these calculations and a summary of the results for each method are presented in Appendix B.

The line of best fit represents the mean of the expected future observations. The variance between the predicted and actual values and the significant wave heights based on the 10 storms hindcast by Marine Advisers (1963) was fit best by Gumbel's first asymptotic distribution. The expected wave height with a 50 percent probability of exceedance is obtained as follows:

$$H = 11.24 + 7.64 \ln (T - .5) \tag{37}$$

where H = the significant wave height in ft

T = the return period in years.

Beyond the 16-year record, the significant wave height with an 87 percent confidence of non-exceedance is 8.7 feet higher than the mean values.

The significant wave heights from the 11 storms hindcast by the Corps of Engineers were fit best by the Weibull distribution. However, the mean wave heights resulting from the Weibull and Gumbel's first asymptotic distributions differed by less than .5 foot through a 100-year return period. Because confidence bands to test the validity of the line of best fit and confidence levels beyond the range of observation are applicable to Gumbel's distribution, it was decided to calculate the design wave from this distribution. The mean expected significant wave height from these storms is given by

$$H = 14.21 + 4.78 \ln (T - .5) \tag{38}$$

where H and T are defined as in equation (37). Beyond the record, 5.4 feet must be added to the mean value to yield wave heights witn an 87 percent confidence of non-exceedance.

Figure 10 and Figure 11 show the lines of best fit for the hindcast data using Gumbel's distribution. Tables 6 and 7 summarize the 25-year and 50-year mean expected wave heights and compare the variance of the fit for each of the five methods employed. These results are presented graphically in Figures 12 and 13.

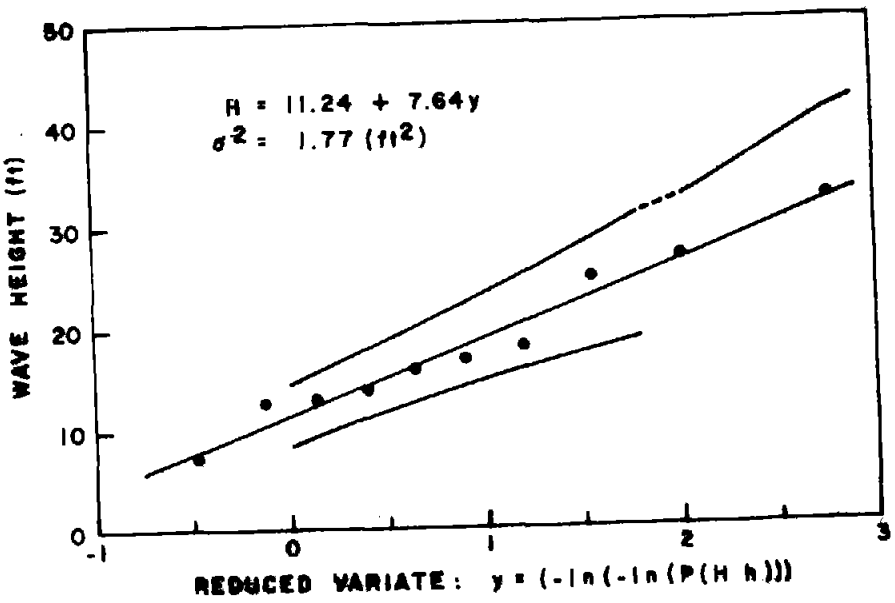

Figure 10. Line of best fit using Gumbel's first asymptotic distribution for significant wave heights from 10 storms affecting the Hawaiian Islands from 1947 through 1961 (Marine Advisers, 1963)

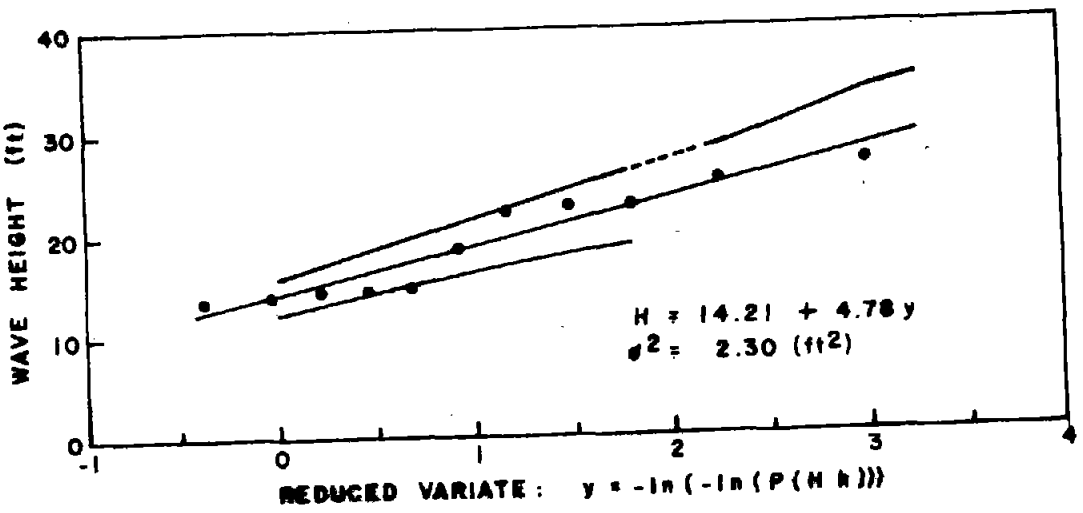

Figure 11. Line of best fit using Gumbel's first asymptotic distribution for significant wave heights from 11 storms affecting Keahole Point from 1947 through 1965 (US Army Corps of Engineers, Honolulu District, 1968)

TABLE 6. MEAN EXPECTED SIGNIFICANT WAVE HEIGHTS WITH A 25 AND 50-YEAR RECURRENCE INTERVAL FOR HAWAIIAN WATERS

Method of Extrapolation	Expected Significant Wave Height (ft)		Variance of the Fit (ft^2)
	25 Year	50 Year	
Normal	29.6	32.0	5.25
Log-normal	32.1	36.8	4.00
Semi-log	38.1	45.3	2.21
Weibull	37.6	43.8	1.94
Gumbel's first	35.7	41.1	1.77

Hindcasts by Marine Advisers, 1964

TABLE 7. MEAN EXPECTED SIGNIFICANT WAVE HEIGHTS WITH A 25 AND 50-YEAR RECURRENCE INTERVAL FOR KEAHOLE POINT

Method of Extrapolation	Expected Significant Wave Height (ft)		Variance of the Fit (ft^2)
	25 Year	50 YEAR	
Normal	26.4	28.1	3.08
Log-normal	27.1	29.6	2.83
Semi-log	30.6	35.1	2.98
Weibull	29.8	33.0	2.12
Gumbel's first	29.5	32.9	2.30

Hindcasts by US Army Corps of Engineers, Honolulu District, 1968

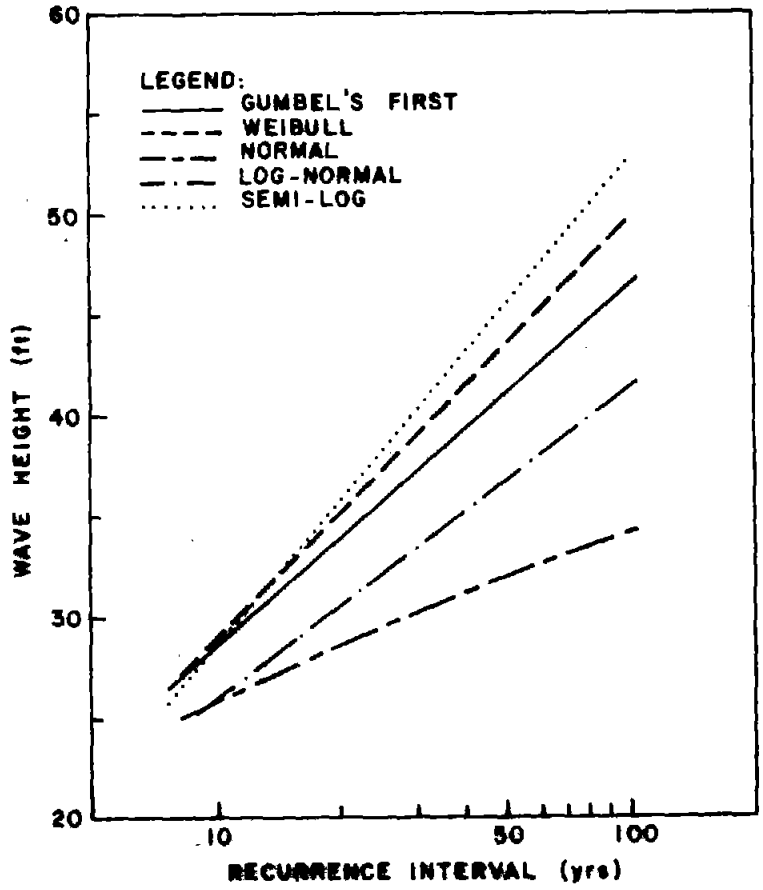

Figure 12. Comparison of the expected wave heights from five methods of extrapolation for 10 storms affecting Hawaii from 1947 through 1961

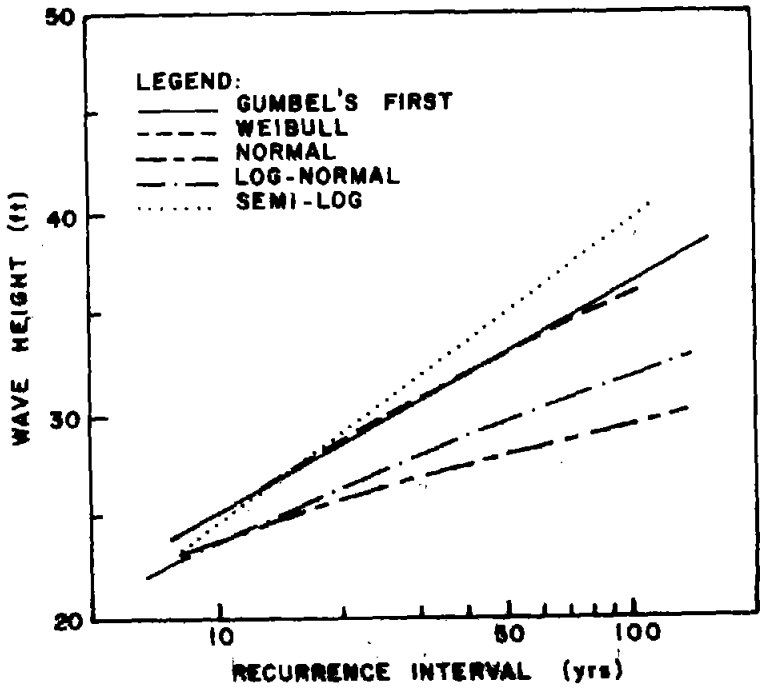

Figure 13. Comparison of the expected wave heights from five methods of extrapolation for 11 storms affecting Keahole Point from 1947 through 1965

The SSMO frequency data were also analyzed using the techniques described in Part I. Based on a review of the Marine Adviser's study of characteristic waves in the Oahu area, 16.5 ft was chosen as the smallest annual maximum of interest. A partial duration series of 34 points was then generated from the SSMO data based on the frequency of occurrence between reported interval end points with a 16.5-foot minimum wave height. For each plot or distribution used, the data within each interval were assumed to be linear along both the ordinate and abscissa. Because of the difficulty of linearizing the probabilities and the previously poor results, the normal and log-normal distributions were not analyzed. The results for the other methods are based on the best fit obtained by least squares analysis. For each method the probability of non-exceedance for an individual event is given by

$$P(H \leq h_m) = 1 - \frac{m}{N + 1} \tag{39}$$

where N = total number of observations = 34

m = rank index of interval endpoint.

The assigned probability of the end points for Gumbel's first asymptotic distribution was calculated assuming each observation to be an independent event. The probability of event h_m being the yearly maximum is then given by (as shown in Part I)

$$P'(H \leq h_m) = P(H \leq h_m)^n \tag{40}$$

where n = number of independent observations per year.

The return period in years is calculated from:

$$T = \exp(y) + 1/2 \tag{41}$$

where $y = -\ln \{-\ln [P'(H \leq h_m)]\}$

For the Weibull distribution and the semi-log plot, the return period in years is

$$T = [1 - P(H \leq h)]^{1/n} \tag{42}$$

To allow calculation of ln (ln T) for the Weibull distribution, the corection to years was made after fitting the data.

The smallest variance for the SSMO partial duration series was obtained using Gumbel's first asymptotic distribution. Confidence bands were calculated using the methods described by St. Denis (1975). Figure 14 shows the line of best fit and confidence bands for Gumbel's first asymptotic distribution. The mean expected wave height based on these shipboard observations is given by

$$H = 23.09 + 2.42 \ln (T - .5). \tag{43}$$

Table 8 summarizes the 25 and 50-year expected wave height and compares the variance of the line of best fit for the three methods used. The results are presented graphically in Figure 15. The 87 percent confidence level is 2.8 feet greater than the mean value given by equation (43) beyond the 8 years of record.

Conclusions

The following conclusions are based on the results of the analysis presented in this section.

1. Gumbel's first asymptotic distribution yields a good fit to extreme wave data including hindcast results and tabulated frequency data if analyzed by the techniques presented here. As the results in Appendix C for seven storms affecting the south side of Keahole Point show, this is valid even with fewer data than theoretically needed to apply the distribution.

2. Using the Marine Advisers' hindcast data, the various methods used resulted in 50-year design waves that were up to 28 percent smaller and 10 percent larger than by the method of minimum variance. The best

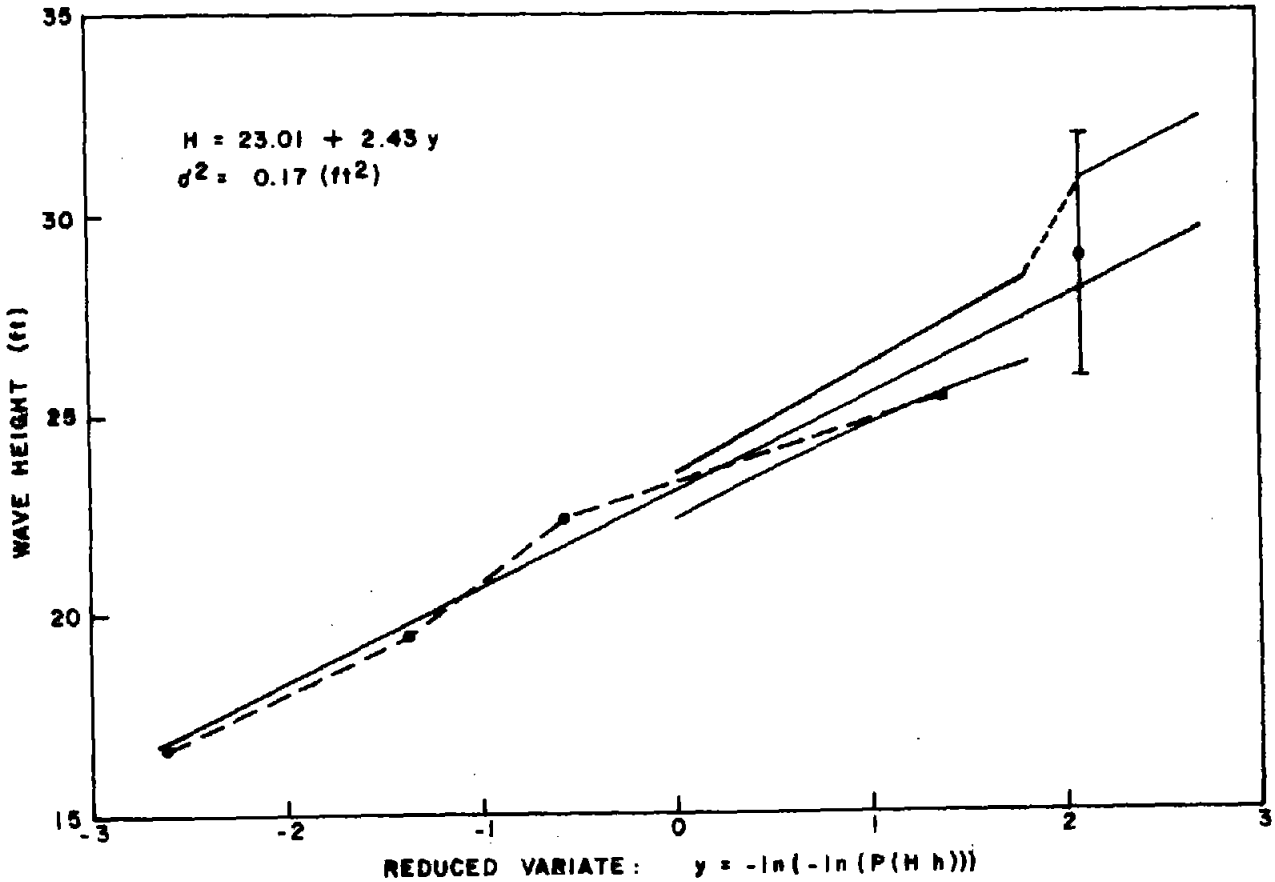

Figure 14. Line of best fit using Gumbel's first asymptotic distribution for 8 years of shipboard observations in SSMO Area 2 (After St. Denis, 1975)

TABLE 8. MEAN EXPECTED SIGNIFICANT WAVE HEIGHTS WITH A 25 AND 50-YEAR RECURRENCE INTERVAL FOR THE AREA LEEWARD OF THE HAWAIIAN ISLANDS

Method of Extrapolation	Expected Significant Wave Height (ft)		Variance of the Fit (ft^2)
	25 Year	50 Year	
Semi-log	32.5	34.8	.583
Weibull	26.2	26.6	.740
Gumbel's first	30.8	32.5	.170

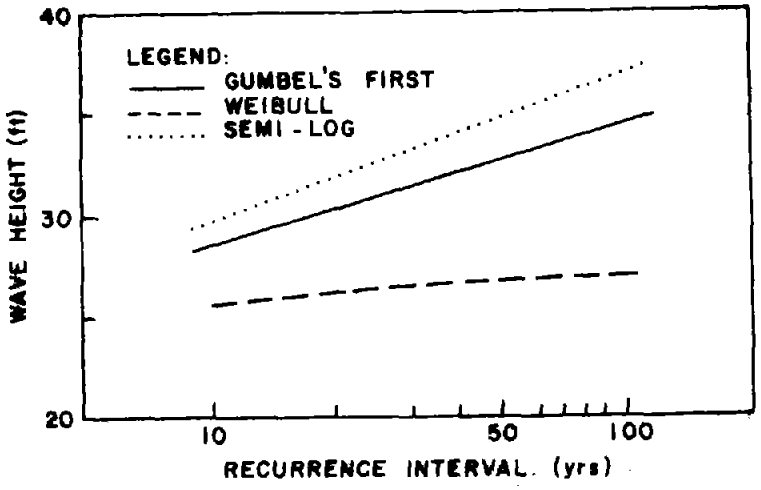

Figure 15. Comparison of the expected wave heights from three methods of extrapolation for the shipboard observations in SSMO Area 2

technique at present is to examine several plotting methods and distributions, choosing that which yields the best fit.

3. Calculation of confidence bands for extreme values of wave height results in significant increases in the design wave. Because of the gross lack of measured data, the use of values at an 87 percent confidence of non-exceedance should be considered. These confidence bands which are not applicable to other methods is another reason for using Gumbel's first asymptotic distribution where possible.

4. Based on fitting Gumbel's first asymptotic distribution to 11 hindcasts specific to western Hawaii and 8 years of shipboard observations in leeward Hawaii, the 50-year significant design wave height is expected to be between 38.3 (32.9 + 5.4) and 35.4 (32.6 + 2.8) feet, with an 87 percent confidence of non-exceedance. Due to the uncertainties in hindcast or visually observed data, a deepwater significant wave height of 38.3 feet will be used to calculate a design storm. This value is considered somewhat conservative for the data specific to Keahole Point, but is still considerably less than the 49.8-foot deepwater significant wave expected to occur once in 50 years somewhere in Hawaiian waters based on the analysis of the Marine Advisers' (1963) hindcast results.

PART III. WINDS

Winds in any area display considerable variation with time, altitude, and specific geographic location. The unsteadiness of wind systems results in rapid temporal variations of substantial magnitude. It is often necessary to include these short-term excursions of peak winds or gust velocities for proper design. One extreme design value often reported is the fastest mile, that is, the fastest wind averaged for a travel distance of one mile. Although various descriptions of the vertical distribution of wind velocity are available, the most commonly used for engineering considerations is the power law given by

$$U_z = U_{10} \left(\frac{z}{10}\right)^m \tag{44}$$

where z = the elevation above the surface in meters

U_z = the wind velocity at height z

U_{10} = the wind velocity at the standard 10-meter reference level

m = the power coefficient which is generally assumed to be 1/7 for design wind speeds.

Topographic features including variations in the surface itself (i.e., land vs water) strongly influence local wind velocities and direction. All these features combine to make it difficult to obtain data specific to individual sites or to extrapolate data from one site to another with great confidence. This problem becomes particularly severe where ocean winds are determined from land-based meteorological facilities.

Wind Climate in Hawaii

The wind climate in the Hawaiian Islands is dominated by the tradewinds which blow out of the northeast to southeast sector. These winds occur approximately 85 percent of the time during the year, being more frequent during the months of April through October when they occur greater than 90 percent of the time. The other significant wind, based on frequency of occurrence, is referred to as kona wind. This name is commonly applied to winds blowing from the southwest quadrant which are present 10 to 15 percent of the time during the winter and infrequently in the summer. Kona winds result from extratropical storm systems associated with the westerlies which are more influential during the winter months when there is a weakening of the easterly wind belt. The intensity of kona winds varies with the strength and location of the storm.

Winds from any quadrant may result from tropical cyclones, commonly known as hurricanes. Although occurring very infrequently, these winds are important because of their high intensity. They gain additional importance since they are often responsible for extreme wave conditions.

Design Wind Data at Keahole Point

The wind climate offshore from Keahole Point is strongly affected by the sheltering effect of Hawaii. Data from the Kailua-Kona airport located near Keahole Point show that the northeast tradewinds are blocked, leading to a high frequency of convective ocean breezes from the west. These breezes tend to be low in velocity and so are not important to design considerations.

Wind velocity records from the Kailua-Kona airport from 1963 through 1974 were examined for extreme values. A change in the location of the recording station in 1970 led to a change in the recorded mean wind speeds and gust speeds. The records from the recent less sheltered location should be more typical of offshore conditions. Unfortunately, the data are not comprehensive enough to yield long-term expected maxima even if corrections for local topography and surface effects are accurately considered.

An estimate of the expected offshore sustained wind speed has been calculated from records of the severe storms affecting western Hawaii. Six storms generating wind seas at Keahole Point have been extrapolated to yield a lower limit on the maximum wind speed expected. Table 9 shows the storms and sustained wind speeds analyzed. It is realized that these wind speeds represent average values which were sustained long enough for wave generation. There is no record of the variation in wind speed about these values during the period of wave generation.

TABLE 9. SUSTAINED WIND SPEEDS FROM STORMS OCCURRING CLOSE TO KEAHOLE POINT

Storm Date	Sustained Wind Speed (knots)
Dec 20, 1955	27
Dec 2, 1957	40
Jan 18, 1959	35
Aug 6, 1959	42
Jan 7, 1962	25
Jan 16, 1963	33

Analysis and Results

Of the 11 storms affecting Keahole Point from the Corps of Engineers' hindcast program, six were close enough to Keahole Point and no decay of the waves had to be assumed. It is therefore reasonable to assume that winds comparable with those used for the hindcasts may have affected the project site. These six values have been analyzed by each of the five methods previously described to extrapolate beyond the record.

Although there are fewer data than theoretically required for the application of Gumbel's first asymptotic distribution, based on the minimum variance, the best fit is obtained with this distribution. The mean expected sustained wind speed as shown in Figure 16 is given by

$$U = 23.22 + 7.21 \ln(T - .5) \tag{45}$$

where T = the return period in years

U = the sustained wind speed in knots.

The confidence bands are not theoretically valid for such a small number of data points; however, based on the slope, variance, and number of points, 8.2 knots added to the mean expected value yields the 87 percent confidence of non-exceedance.

The expected sustained wind velocities for each method are summarized in Table 10 and Figure 17.

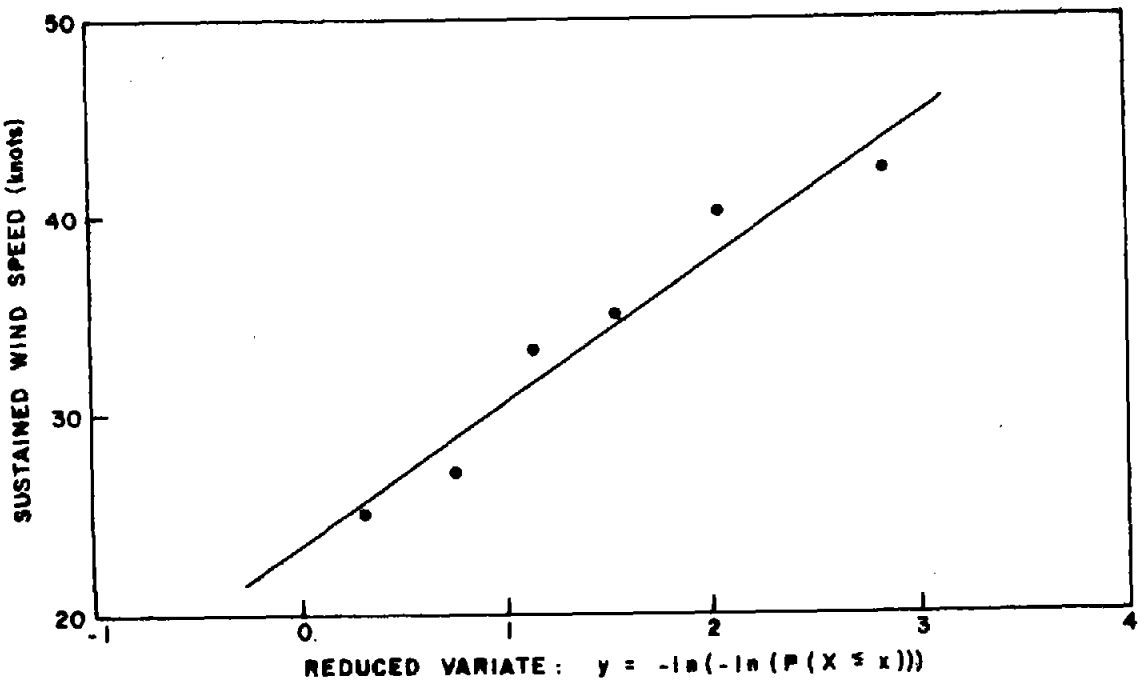

Figure 16. Line of best fit using Gumbel's first asymptotic distribution for sustained winds affecting Keahole Point

TABLE 10. MEAN EXPECTED SUSTAINED WIND SPEED WITH A 25 AND 50-YEAR RECURRENCE INTERVAL FOR KEAHOLE POINT

Method of Extrapolation	Expected Sustained Wind Speed (knots)		Variance of the Fit (knots^2)
	25 Year	50 Year	
Normal	41.4	43.7	4.21
Log-normal	41.9	44.9	4.24
Semi-log	47.2	53.9	4.03
Weibull	47.2	52.7	2.98
Gumbel's first	46.3	51.3	2.03

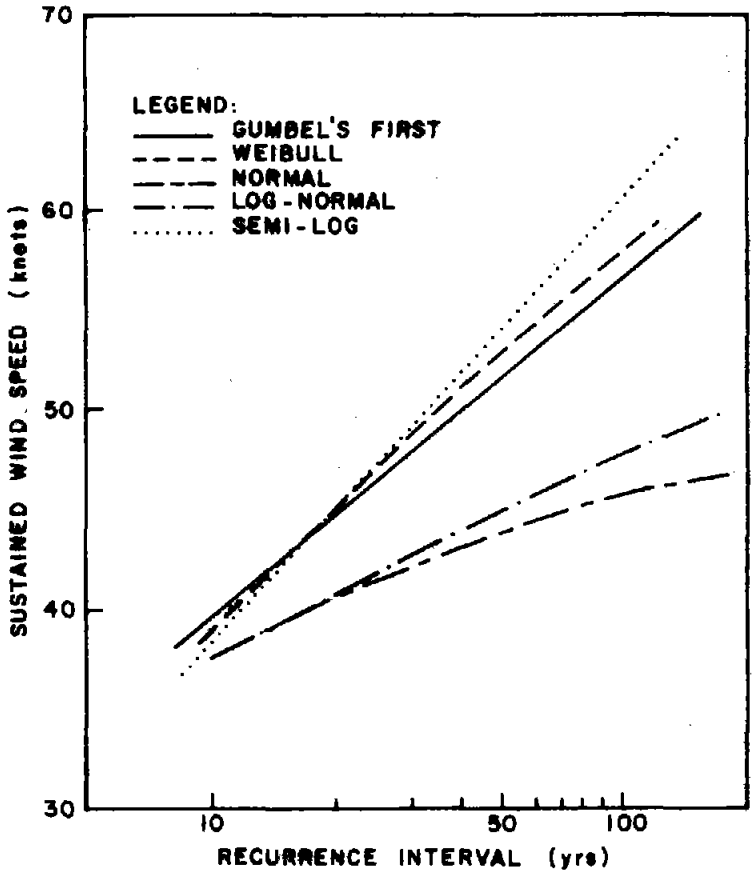

Figure 17. Comparison of the expected wind speeds from five methods of extrapolation

Conclusions

The results of the analysis for design wind velocities support the following conclusions made based upon the wave analysis:

1. Gumbel's first asymptotic distribution, although not theoretically valid for so small a data base, yields the best fit to hindcast extreme wind conditions compared with other commonly used methods.

2. Large differences in design wind velocities occur with the choice of plotting method. Differences of up to 15 percent of the chosen 50-year design wind were obtained using the same data.

3. Based upon fitting Gumbel's first asymptotic distribution to hindcasts specific for western Hawaii, the 50-year sustained wind velocity is expected to be at least 59.5 (51.3 + 8.2) knots.

PART IV. RUN-UP FOR SELECTED TRANSECTS AT KEAHOLE POINT

Design wave and wind conditions for unprotected deepwater projects such as the proposed ocean thermal energy conversion plant are given in the previous sections. However, shallow water and shore-based facilities will be subject to a modified wave climate or possible damage due to run-up beyond the shoreline. This section deals specifically with the inundation levels expected to occur due to wind waves during the design storm for selected transects at Keahole Point. Determination of the wind wave run-up depends on an accurate description of the still water level (SWL) over which the design wave passes and the changes in wave characteristics close to shore due to refraction, shoaling, and breaking.

Design Water Level

The water depth at the shoreline and in front of a coastal structure directly influences the characteristics of approaching waves. For many locations, the maximum wave height which may impinge on the structure is limited by depth and bathymetry. Together with the deepwater wave climate this determines the maximum non-breaking or largest breaking wave which will be encountered. Since the maximum wave is approximately proportional to the water depth, accurate determination of the depth is critical.

The total water depth is given by Bretschneider (1973a) as:

$$d_T = d_o + A_S + z_o + S_x + S_y + \eta + \alpha H_b \qquad (46)$$

where d_T = total design water depth

d_o = reference water level

A_S = astronomical tide

z_o = forerunner to storm

S_x = water setup due to wind stress perpendicular to the coast

S_y = water setup due to wind stress parallel to the coast

η = sea level rise due to a reduction in atmospheric pressure

H_b = breaking wave height

α = about 10 to 20 percent

αH_b = wave setup.

Second order coupling among individual components, complex bathymetry, and uncertain storm history makes determination of the water depth as a function of time difficult. However, for design estimates the level may be calculated by the linear addition of individual component maxima. The magnitudes expected for each at Keahole Point are shown below.

Reference water depth

Depth measurements around Keahole Point relative to mean lower low water were obtained from US Coast and Geodetic Survey chart 4140. Soundings from close to shore to the 300-fathom depth were obtained by a field team from R.M. Towill Corporation using a Raytheon Precision fathometer. Three runs at headings 226°T, 266°T, and 246°T from the point were made and the depth at shore for each run was determined. The results showing the distance from shore and the depth to the first sublayer as summarized by Bathen (1975) are presented in Tables 11, 12, and 13.

Astronomical tide

Astronomical tide is the periodic fluctuation of the water level which results from a balance of centrifugal forces and the gravitational attraction of the earth with the moon and sun. Tides in Hawaii are predominantly mixed semidiurnal, with two unequal highs and lows daily. Tide tables from the NOAA publications report a diurnal range of 2.1 feet along the west coast of Hawaii. This value is the average difference in height between the mean higher high water and mean lower low water, the datum plane for water level calculations in this report. For a somewhat conservative design it is better to use a water level closer to the extreme high water level. Examination of several years' tide tables shows

TABLE 11. FATHOMETER DATA FROM KEAHOLE POINT AT 226°T

Scale on Trace	Distance (ft)	Depth (fathoms)	Scale on Trace	Distance (ft)	Depth (fathoms)
0.00	0	4.0/5.5	7.72	3,000	136.5
0.26	101	6.0/7.0	8.12	3,155	147.8
0.38	148	9.0	8.38	3,255	153.8
0.72	280	17.5	8.63	3,355	158.3
0.78	303	20.0	8.83	3,430	165.5
1.20	466	36.0	9.32	3,620	174.5
1.27	494	38.5	9.53	3,705	185.0
1.28	498	40.0	9.72	3,780	195.0
1.78	691	45.0	10.21	3,970	212.5
1.89	735	46.8	10.28	3,990	215.8
1.94	754	46.5	10.42	4,055	223.0
2.17	843	48.3	10.60	4,120	229.0
2.27	882	49.5	10.79	4,190	234.5
3.38	1,311	49.5	10.94	4,255	235.0
3.93	1,526	50.0	11.11	4,320	248.0
4.37	1,695	50.8	11.17	4,340	247.5
4.77	1,850	53.5	11.34	4,410	253.8
5.13	1,992	55.0	11.50	4,465	256.3
5.37	2,085	59.8	11.76	4,570	265.0
5.93	2,300	67.3	12.11	4,710	283.0
6.02	2,340	71.0	12.50	4,855	296.0
6.14	2,382	77.0	12.70	4,940	301.5
6.23	2,415	79.8	12.93	5,030	309.5
6.41	2,487	86.8	13.40	5,205	319.2
6.62	2,570	98.3	13.45	5,225	323.5
6.85	2,660	108.8	13.61	5,295	324.0
7.08	2,750	119.3	13.75	5,345	330.0
7.15	2,775	123.8	14.15	5,500	338.5
7.31	2,840	129.0	14.42	5,600	351.0
7.49	2,905	133.0			

Source: Bathen, 1975

TABLE 12. FATHOMETER DATA FROM KEAHOLE POINT AT 266°T

Scale on Trace	Distance (ft)	Depth (fathoms)	Scale on Trace	Distance (ft)	Depth (fathoms)
0.00	0	3.0/4.0	4.07	2,760	106.5
0.09	61	2.3/3.5	4.13	2,800	109.3
0.11	75	3.5/4.5	4.31	2,920	122.3
0.25	169	3.8/4.8	4.44	3,005	132.5
0.45	305	7.0/8.0	4.55	3,080	136.3
0.87	589	18.5/19.8	4.75	3,220	144.5
0.89	603	17.8/19.3	4.97	3,370	153.0
0.95	643	24.0	5.15	3,490	166.5
0.97	657	25.0/25.5	5.33	3,605	176.5
0.98	664	26.5	5.57	3,775	186.5
1.05	721	29.5	5.80	3,930	194.5
1.09	738	33.5	5.95	4,030	198.3
1.52	1,030	41.3/42.5	6.12	4,150	203.8
1.69	1,147	44.5/45.5	6.21	4,210	208.3
2.03	1,375	53.0/54.0	6.26	4,245	213.8
2.76	1.870	58.7/59.5	6.33	4,290	212.9
3.25	2,200	62.8/64.0	6.37	4,320	216.6
3.46	2,245	66.5/67.0	6.45	4,370	215.3
3.57	2,420	69.0	6.88 (D)	4,655	250.8
3.65	2,475	73.5	7.20 (D)	4,875	271.3
3.67	2,487	75.5	7.56 (D)	5,125	287.3
3.72	2,520	78.0	7.78 (D)	5,265	301.3
3.82	2,585	86.0	7.93 (D)	5,370	(320.0)
3.87	2,620	91.5	8.21 (D)	5,560	(340.0)
4.02	2,720	102.0	8.42 (D)	5,700	(351.0)

Source: Bathen, 1975

Note: (D) = doubtful depth; (320.0), (340.0), and (351.0) = estimated depths

TABLE 13. FATHOMETER DATA FROM KEAHOLE POINT AT 246°T

Line Number	Distance (ft)	Depth (fathoms)	Line Number	Distance (ft)	Depth (fathoms)
0	0	3.5	664	2,515	91.5
12	46	3.8	678	2,570	95.5
24	91	4.5	701	2,660	105.0
34	129	5.0	713	2,700	109.5
46	174	7.0	718	2,720	113.0
58	220	10.0	725	2,745	115.5
75	284	14.5	737	2,795	119.5
93	352	20.0	754	2,855	126.5
107	406	23.5	769	2,920	133.0
122	462	28.5	782	2,965	139.8
139	526	35.5	796	3,020	143.5
153	580	38.0	800	3,035	146.0
166	629	40.2	811	3,075	147.0/149.0
182	690	43.0/44.4	826	3,130	152.0/155.0
195	739	44.5/45.5	832	3,150	155.5/157.0
212	804	47.0/48.3	844	3,200	161.0
227	860	49.2/50.7	853	3,230	163.0
244	925	51.8/53.0	855	3,240	163.0/169.5
264	1,000	53.8/55.0	858	3,252	163.5/167.0
286	1,083	54.4/55.2	863	3,270	165.0
306	1,160	54.8/56.0	874	3,310	168.2
327	1,240	55.5/57.0	881	3,340	170.0
330	1,250	56.0/57.2	891	3,380	173.8
333	1,261	55.5/56.8	912	3,455	178.8
349	1,323	56.0/57.0	936	3,550	189.5/193.0
370	1,403	57.0/58.0	952	3,608	195.8/198.5
387	1,468	57.2/58.4	971	3.680	204.0
402	1,522	57.8/59.0	979	3,710	208.0
422	1,600	58.2/59.8	1,015	3,840	219.8
454	1,720	59.0/60.0	1,045 (N)	3,960	227.8/235.0
470	1,781	59.8/61.0	1,084 (N)	4,110	242.8/249.0
487	1,849	60.0/61.8	1,101 (N)	4,170	250.0/253.5
510	1,932	62.8/63.0	1,128 (N)	4,260	259.5/264.0
526	1,995	63.0/63.8	1,163 (N)	4,420	269.0/272.0
539	2,040	63.8	1,189	4,500	278.0
560	2,122	65.5	1,226	4,650	288.8
581	2,200	69.0	1,263	4,785	301.0
595	2,258	71.8	1,270	4,815	303.8
607	2,300	74.0	1,276	4,840	304.8
623	2,360	77.0	1,294	4,905	310.0
633	2,400	81.0	1,310	4,960	315.0
638	2,420	83.0	1,330	5,045	322.5
642	2,435	82.5	1,350	5,120	327.0
654	2,480	87.0			

Source: Bathen, 1975

Note: (N) = nebulous distinction between strata

that a maximum high tide of 2.8 feet or greater occurs 1.4 percent of the days and 2.7 feet or greater 5.5 percent of the days. The design water level is based on a tidal magnitude of 2.7 feet. This is in agreement with Walker (1969) who estimated a 2.5-foot astronomical tide for the design of the Honolulu Reef Runway Project.

Forerunner

The forerunner is a rise in sea level which precedes the effects of the wind tide. Since no suitable analytical method for the calculation of the forerunner was found and since no effects of hurricanes have been accurately recorded for this area, the forerunner is assumed to be negligible for these preliminary run-up calculations.

Pressure tide

In case of a hurricane, there is a rise in sea level caused by a reduction in atmospheric pressure given by:

$$\eta = 1.14\ K\ \Delta P\left(1 - e^{-R/r}\right) \tag{47}$$

for $R \leq r$

where η = sea level rise in ft

ΔP = reduction in atmospheric pressure in inches of mercury in the hurricane center

K = a response factor

$\left(1 - e^{-R/r}\right)$ = correction to central pressure drop with radius.

The pressure response is given by

$$K = gd/\left(gd - V_a^2\right) \tag{48}$$

where V_a = forward velocity of the pressure front

d = depth of the water

Equation (48) shows that as the speed of the storm approaches the shallow water wave velocity $(gd)^{1/2}$, resonance effects are likely. For a storm moving at the design speed of 12 knots, the critical depth is 13 feet. This is less than any measured depth off Keahole Point. Together with the steep bottom slope and the probable path of the storm parallel to or away from the coast, a pressure response factor of 1.0 is justified. Assuming ΔP = 1.0 inches of mercury, the 50-year design pressure tide at the location of maximum wave generation is

$$\eta = 1.14\ (1.0)(1.0)\left(1 - e^{-.5}\right) = 0.45\ \text{ft.} \tag{49}$$

Setup due to wind stress

Wind blowing at an angle to the coastline results in a wind tide consisting of two components. The first is due to wind stress on the surface acting normal to the coastline. The second results from stress acting parallel to the coast which creates a shoreward component due to the Coriolis effect.

Although very important in areas with a wide continental shelf, the setup due to wind stress is negligible where a depth of 100 fathoms is reached within 2,700 feet from shore, as is the case at Keahole Point. Because the wind stress was expected to yield an insignificant tide, several simplifying assumptions were made to yield a preliminary estimate. These assumptions include:

1. Of the three bathymetric profiles, the transect at 266°T which had the most gradual gradient was used. The slope was assumed to be constant to the depth of interest. The second of these profiles is conservative for a shelf which drops off more rapidly near shore as at Keahole Point.

2. Although the winds decrease radially from the center of the hurricane, a sustained wind equal to the maximum sustained speed was used. This is again a conservative assumption.

3. Steady state was assumed.

These approximations and the bathystrophic approximations described by Bretschneider (1967) allow a simple estimate of the wind tide to be made.

Integration of the equations of motion with substitution of the bathystrophic conditions and the relationships between the surface and bottom stresses with wind velocity and bottom flow as described by Bretschneider (1967) yields the following governing equations:

$$S_x = \frac{k\, U^2\, X \cos\Theta}{g[D_o - (D + S)]} \ln \frac{D_o}{(D + S)} \tag{50}$$

$$S_y = \frac{6}{7} \frac{fUX}{g} \left(\frac{k}{k} \sin\Theta \right)^{1/2} \frac{D_o^{7/6} - (D + S)^{7/6}}{D_o - (D + S)} \tag{51}$$

$$S = S_x + S_y \tag{52}$$

where S_x = wind tide due to normal wind component (ft)

S_y = wind tide due to parallel wind component (ft)

U = wind speed (ft/sec)

X = distance over which wind stress is important (ft)

D_o = seaward depth at edge of shelf (ft)

D = mean depth at shoreward end of shelf (ft)

S = surge height at any location (ft)

f = Coriolis parameter

k = constant relating wind velocity to surface stress

k = constant relating fluid flow to bottom stress ($ft^{1/3}$)

Θ = angle of wind to coastline.

For any particular wind speed and direction, the wind tide will be a maximum when X and D_o are chosen such that the group of variables

$$G = \frac{X}{D_o - (D + S)} \ln \frac{D_o}{(D + S)} \tag{53}$$

are maximum. In the evaluation of G, (D + S) is chosen seaward of the coast or structure before the final increase in slope to the shoreline. The values of D_o and X are then chosen by trial and error from the bathymetric profiles.

Examination of the bathymetric profiles reported by Bathen (1974) shows that a suitable value of (D + S) is approximately 26.0 feet including the astronomical tide and pressure tide. Using actual depths reported in Table 11 but assuming a constant slope results in a maximum value of G when the seaward depth is 69 fathoms at a distance of 2,420 feet from shore. Regardless of the wind speed and direction, the wind tide is found to be negligible for design at Keahole Point.

Wave setup

Although waves breaking offshore will result in setup due to the change in momentum flux, this value does not need to be included in the design water level for the calculation of wave run-up presented below. Run-up is based on deepwater wave parameters, the geometry of the shoreline, and the still water level.

Wave Run-up Estimation for Selected Transects

An estimation of wave run-up and inundation levels for selected transects at Keahole Point has been made to provide guidance in the positioning of instruments and instrument houses and to determine the need for protective structures for permanent facilities.

Calculated wave run-up for other than smooth sloping beaches and standard coastal structures are subject to considerable engineering judgment and are approximate at best. This is certainly the case for the irregular shoreline and topography at Keahole Point.

Numerous publications have discussed the run-up of non-breaking waves on sloping surfaces. Breaking waves have been described using non-linear long wave theory assuming propagation as a bore, but the procedures tend to be very specific in applicability. In addition to the theoretical work, experimental measurements of wave run-up have been carried out for a variety of shorelines and structures. A descriptive summary of several theories and much of the experimental work have been assembled by Battjes (1972).

Much of the design work in the United States is based on the results of experiments conducted with regular waves by Saville (1956). The results of Saville, tabulated in the CERC *Shore Protection Manual*, present run-up as a function of surface slope and deepwater wave parameters. An empirical extension of these results for the calculation of run-up on a non-plane slope called the equivalent gradient method was also presented by Saville. The equivalent slope is determined by the intersection of the plane slope and the non-plane slope at the position of the wave breaking and the location of maximum run-up. In the absence of a more suitable method, this method has been applied at Keahole Point.

Model tests by Hensen (1955) show good agreement with the equivalent gradient method for plane and for convex slopes; however, the calculated run-up is somewhat low for concave slopes in this comparison. In addition, berm widths greater than one-seventh of the wave length continue to decrease the run-up but less rapidly than as calculated by Saville's (1956) method. These possible sources of error, and the very irregular topography causing local divergences and convergences of the flow, allow only a preliminary estimate of the run-up to be made for Keahole Point.

The influence of roughness and permeability also needs to be considered in the estimation of run-up. Their effect is complex and coupled so that a combined reduction factor $\underline{r}$ is normally reported. Typical values from several sources are shown in Table 14.

TABLE 14. RUN-UP REDUCTION FACTORS FOR ROUGH PERMEABLE SURFACES

Source	Surface Covering	Permeability Coefficient (r)
--	Smooth impermeable surface	1.00
CERC, 1973	1 layer of rubble	0.80
CERC, 1973	2 or more layers of rubble	0.50 to 0.55

Transects for which run-up estimates were made are shown in Figure 18. All transects were chosen to be near the temporary generator house presently in use. Profiles for transects 1 through 5, taken from the *Topographic Map of the Keahole Point Area* published by the Natural Energy Laboratory of Hawaii, are shown in Figures 19 and 20. The still water level was taken as 21 feet plus 2.7 feet for high tide plus .5 foot for the pressure tide at the waterline. Estimations of the run-up for long period swells were made without the .5-foot pressure tide. The offshore bathmetry reported by Bathen (1974) shows a bottom slope of approximately 1:6 in the nearshore region. Breaking wave heights and depths at the break point were determined from figures in the *Shore Protection Manual* (CERC, 1973). Run-up for four short-period storm waves and two long-period swells were calculated for transect 1. Calculations for only one short-period wave and one swell were made for the remaining transects. The results are summarized in Table 15.

The results show that waves even considerably smaller than the 50-year significant design wave may cause flooding or damage due to run-up in the location of the temporary generator house. Although local divergences and convergences of the flow may substantially alter the run-up at specific sites, the generator house site is fronted by terrain which is not expected to drastically alter the flow. Transects 1, 2, 4, and 5 (Figure 18) approach nearly normal to the local contours.

The run-up from the long-period swell calculated by the technique given in the *Shore Protection Manual* (CERC, 1973) appears reasonable when compared with actual observations. In the winter of 1975, during the construction of the generator house, run-up from large swell damaged one wall at an elevation of approximately 12 feet at a distance of about 300 feet from the shoreline.

Before construction of permanent facilities, a model testing run-up in the area would be desirable. Before such a study, however, it would be necessary to more accurately map the nearshore bathymetry for refraction analysis to determine those shoreline areas most prone to large wave attack.

The work of Wybro (1976: personal communication) showed that the run-up of the 100-year tsunami is considerably more important for design purposes than that due to storm waves. The 100-year tsunami is expected to run-up to a vertical elevation of 15.0 feet at Keahole Point with an inland inundation of 1,200 feet. However, run-up of lesser heights due to storm waves occur more frequently and should therefore be considered for maintenance design costs.

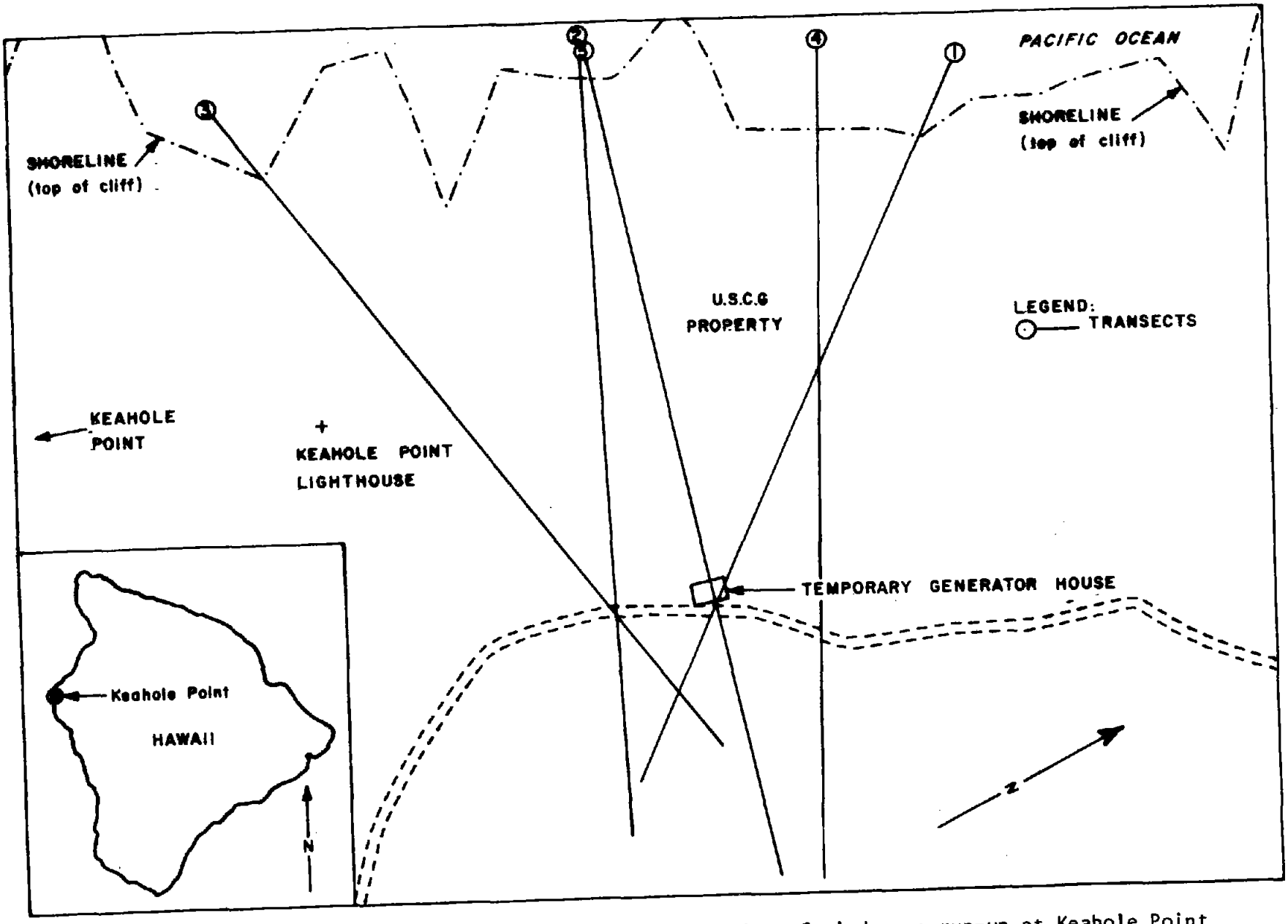

Figure 18. Location of five transects for the calculation of wind wave run-up at Keahole Point (After Bathen, 1975)

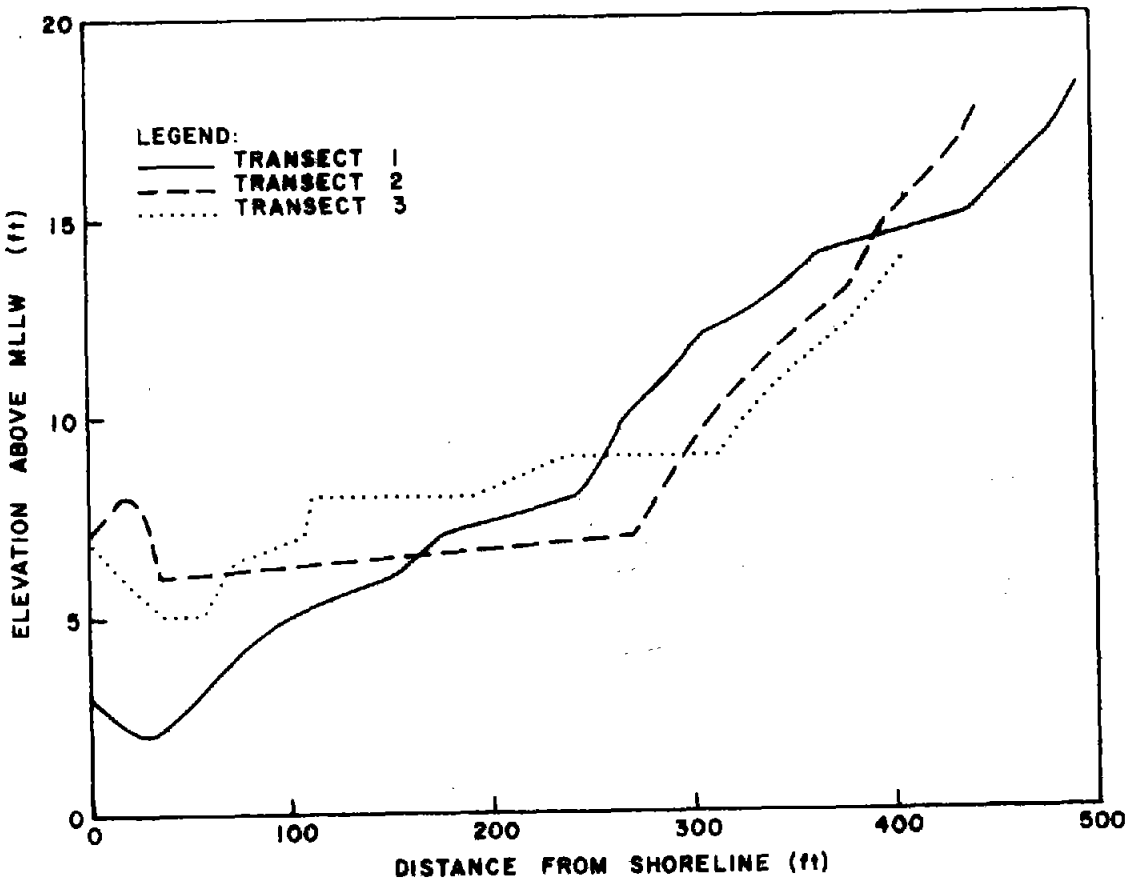

Figure 19. Profiles of transects 1, 2, and 3 at Keahole Point

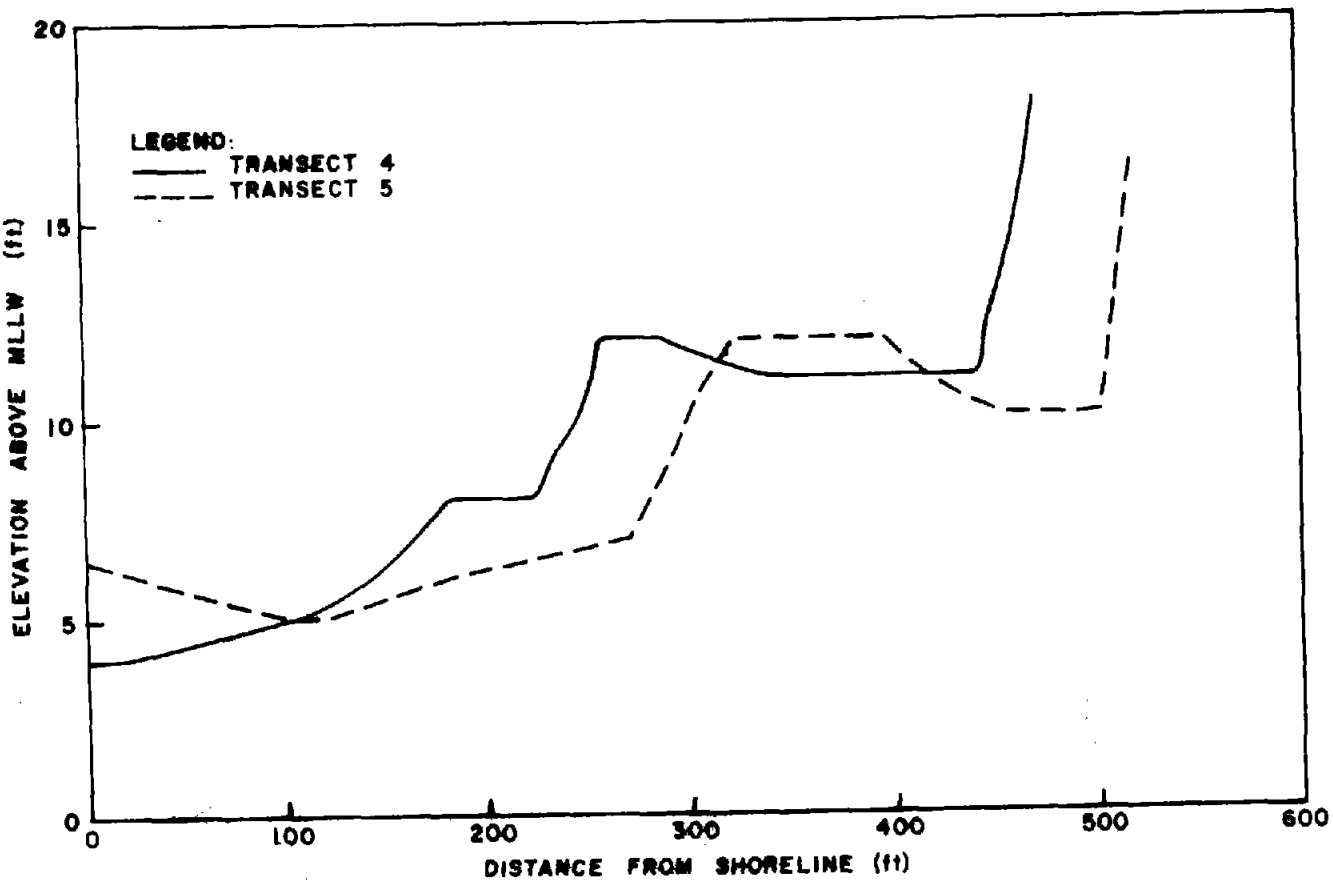

Figure 20. Profiles of transects 4 and 5 at Keahole Point

TABLE 15. SUMMARY OF WIND WAVE RUN-UP FOR SELECTED TRANSECTS AT KEAHOLE POINT

Transect Number	Transect Direction (°T)	Deep Water Wave Height (ft)	Wave Period (sec)	Run-up Elevation Above MLLW (ft)	Inundation (ft)
1	328	38.3	12.5	16.5	470
1	328	32.9	12.5	15.0	440
1	328	29.5	12.5	14.5	405
1	328	25.0	12.0	14.0	365
1	328	25.0	15.0	15.0	440
1	328	20.0	17.0	15.0	440
2	293	25.0	12.0	13.5	382
2	293	20.0	17.0	15.0	400
3	259	25.0	12.0	13.5	400
3	259	20.0	17.0	> 14.0	> 400
4	284	25.0	12.0	12.0	447
4	284	20.0	17.0	14.0	458
5	298	25.0	12.0	11.5	505
5	298	20.0	17.0	12.0	508

LIST OF SYMBOLS

a	Arbitrary constant
b	Arbitrary constant
a_n	Constant based on sample size and the shape of the distribution of interest
b_n	Constant based on sample size and the shape of the distribution of interest
A	Lower limit of the variable in the Weibull distribution
B	Scale factor in the Weibull distribution
C	Shape factor in the Weibull distribution
f_r	Aggradation factor relating significant to maximum wave height
$F(X)$	Probability distribution function of the random variable X
H_s	Significant wave height
m	Rank of observed values of the random variable X
m_o	Mean square value of the wave elevation
M	Total number of events
n	Number of events per unit of time
L	Design life in years
N	Number of years or design life
$P(X \leq x_m)$	Probability of an event X being less than or equal to x_m
$P'(X \leq x_m)$	Probability of n independent trials all being less than or equal to x_m
r	Number of trials, also permeability coefficient
R	Probability of failure
T	Return period
T_y	Expected return period of event x_m being the yearly maximum
T_m	Expected return period of event x_m in years
U	Arbitrary constant ≥ 1
X	Variable of interest
y	Reduced variate in extremal distributions
z	Elevation above the surface
$\xi_{1/n}$	Amplitude of the 1/nth highest wave
$\bar{\xi}_{1/n}$	Average amplitude of the highest 1/n observations
τ	Time between events
α, μ	Parameters of Gumbel's first asymptotic distribution
$\hat{x}$ μ, k	Parameters of Gumbel's third asymptotic distribution

REFERENCES CITED

American Society of Civil Engineers, Hydraulics Division. 1958. *Hydrology Handbook.* ASCE, New York.

Bathen, K.H. 1975. *An Evaluation of Oceanographic and Socio-Economic Aspects of a Nearshore Ocean Thermal Energy Conversion Pilot Plant in Subtropical Hawaiian Waters.* Report submitted to National Science Foundation. Department of Oceanography, University of Hawaii, Honolulu. pp. 3.2-1 - 3.2-92.

Battjes, J.A. 1972. *Long Term Wave Height Distributions at Seven Stations Around the British Isles.* Deutsche Hydrographische Zeitschrift.

Beard, R.L. 1952. *Statistical Methods in Hydrology.* US Army, Office of Chief of Engineers.

Bretschneider, C.L. 1965. *Generation of waves by wind: state of the art.* Tech. Report SN 134-6. National Engineering Science Co.

Bretschneider, C.L. 1967. "Storm surges." *Advances in Hydroscience.* New York: Academic Press Inc. 4:341-417.

Bretschneider, C.L. 1973a. *Design hurricane waves for the Island of Oahu, Hawaii with special application to Sand Island Ocean Outfall System.* Look Lab/Hawaii, Vol. 3, No. 2.

Bretschneider, C.L. 1973b. "A tentative analysis of wave data for design wave criteria around Taiwan." *Acta Oceanographica Taiwanica* (3):1-23. Science reports of the National Taiwan University, December, 1973.

Brooks, R.L., and N.H. Jasper. 1957. *Statistics on wave heights and periods for the North Atlantic Ocean.* Report no. 1091. David Taylor Model Basin, Washington, D.C.

Cartwright, D.E. 1964. *The presentation and wave data from voluntary observing ships.* NPL Ship Report no. 49.

Court, A. 1952. "Some new statistical techniques in geophysics." *Advances in Geophysics.* Vol. 1. New York: Academic Press, Inc.

Darbyshire, J. 1961. "Prediction of wave characteristics over the North Atlantic." *Journal of the Institute of Navigation.* London, England

Draper, L. 1963. "Derivation of a 'design wave' from instrumental records of sea waves." In *Proceedings of the Institute of Civil Engineers, London, England.* Vol. 26. pp. 291-304.

Fisher, R.A., and L.H.C. Tippet. 1928. "Limiting forms of the frequency distribution of the largest or smallest member of a sample." In *Proceedings of the Cambridge Philosophical Society.* Vol. 24. pp. 180.

Gumbel, E.J. 1958. *Statistics of Extremes.* New York: Columbia University Press.

Hensen, W. 1955. "Modellversuche mit pneumatischen wellenbrechern." *Mitt Hannoverschen Versuchsanst.* 7:179-212.

Hogben, N., and F.E. Lumb. 1967. *Ocean Wave Statistics.* Ministry of Technology. National Physical Laboratory, England.

Inman, D.L., W.R. Gayman, and D.C. Cox. 1963. "Littoral Sedimentary Process on Kauai, a Sub-tropical High Island." *Pacific Science* XVII(1):

Jasper, N.H. 1956. "Statistical distribution patterns of ocean waves and wave induced ship stresses and motions with engineering applications." In *Transactions, Society of Naval Architects and Marine Engineers.* Vol. 64. pp. 375-432.

Khanna, J., and P. Andru. 1974. "Lifetime wave height curve for Saint John Deep Canada." In *International Symposium on Ocean Wave Measurement and Analysis,* American Society of Civil Engineers. Vol. 1. pp. 301-319.

Langbein, W.B. 1949. "Annual floods and partial duration series." In *Transactions, American Geophysical Union.* 30(6):879-881.

Longuet-Higgins, M.S. 1952. "On the statistical distribution of the heights of sea waves." *Journal of Marine Research.* 11(3):

Marine Advisers. 1963. *Severe Storm Wave Characteristics in the Hawaiian Islands.* Marine Advisers, La Jolla, California. Prepared for Board of Harbor Commissioners, Transportation Department, State of Hawaii.

Marine Advisers. 1964. *Characteristics of Deep-Water Waves in the Oahu Area for a Typical Year.* Marine Advisers, La Jolla, California.

Mayencon, R. 1969. "Etude statistique des observations de vagues." *Cahiers Oceanographiques.* 21:487-501. In French.

Moberly, R., and T. Chamberlain. 1964. *Hawaiian beach systems.* Prepared for the Harbors Division, Department of Transportation, State of Hawaii. Also HIG-64-2. Hawaii Institute of Geophysics, University of Hawaii, Honolulu.

Nordenstrom, N. 1969. "Methods for predicting long term distributions of wave loads and probability of failure for ships. Appendix II. Relationship between visually estimated and theoretical wave heights and periods." Det Nonske Veritas, Research Dept. Report no. 69-22-5. Oslo.

St. Denis, M. 1974. *Hawaii's Floating City Development Program: the winds, currents, and waves at the site of the floating city off Waikiki.* UNIHI-SEAGRANT-CR-75-01, University of Hawaii Sea Grant College Program, Honolulu. Also Technical Report No. 8, Oceanic Institute, Waimanalo.

St. Denis, M. 1975. "On statistical techniques for predicting the extreme dimensions of ocean waves and of amplitudes of ship responses." Paper presented at First Ship Technology and Research Symposium, Washington, D.C.

Saville, T., Jr. 1956. "Wave runup on shore structures." *Journal of the Waterways and Harbors Divisions.* WW2. Vol. 82. American Society of Civil Engineers.

US Air Force, Air Research and Development Company. 1961. *Handbook of Geophysics.* New York: The MacMillan Company.

US Army Coastal Engineering Research Center. 1973. *Shore Protection Manual.* Washington, D.C.: US Government Printing Office. In three volumes.

US Army Corps of Engineers, Honolulu District. 1968. General Design Memorandum-Honokohau Harbor for Light Draft Vessels. Honolulu.

US Navy Weather Service Command, National Technical Information Service. 1971. *Summary of Synoptic Meteorological Observations.* Springfield, Virginia.

Walker, J.R. 1969. *Three-Dimensional Storm Wave Study, Reef Runway Hydraulic Model Study.* Look Lab TR-8. Look Laboratory of Oceanographic Engineering, Department of Ocean Engineering, University of Hawaii. 137 pp.

Weibull, W. 1951. "A statistical distribution function of wide applicability." *Journal of Applied Mechanics.* 18:293-297.

Whittingham, H.E. 1964. *Extreme Wind Gusts in Australia.* Bulletin No. 46. Bureau of Meteorology. 133 pp.

APPENDICES

Appendix A. Procedures for Application of Gumbel's Distributions (From St. Denis, 1975)

1. Gumbel's first asymptotic distribution

   a. Order the inputs, assigning a rank (m) from the largest to smallest value:

$$x_1 > x_2 > x_3 > \ldots > x_m.$$

   b. Calculate the cumulative probability and reduced variate for each observation:

$$P(X \leq x_m) = F(x_m) = 1 - \frac{m}{M + 1}$$

$$y_m = -\ln[-\ln F(x_m)].$$

   c. Plot x_m versus y_m. Determine the slope $(1/\alpha)$ and the model value (μ) by least squares analysis:

$$x = \mu + y/\alpha.$$

   d. Calculate the confidence bands around the central values. These values are those associated with a reduced variate (y_m) less than 1.82. The confidence bands are located on either side of the ordinate at a distance:

$$\Delta X = \pm[f(p)/\alpha \sqrt{m}]n$$

   where $f(p) = \sqrt{1/p - 1} \; / \; (-\ln P)$

   n = the number of standard deviations

   $p = \exp[-\exp(-y)]$

   m = the number of events.

   e. Calculate the confidence bands about the extreme points (m = 1, 2, 3, 4). These confidence bands are located on either side of the theoretical value of x_m at a distance determined by the following table.

TABLE A-1. PROBABILITY OF CONTAINMENT

Interval	ϕ = .6827(1σ)	ϕ = .9545(2σ)
ΔX_1	1.14078/α	3.0669/α
ΔX_2	.75409/α	1.7820/α
ΔX_3	.58900/α	1.3500/α
ΔX_4	.53800/α	1.1700/α

f. Connect the 1σ and 2σ confidence bands over the range of data. If 68.3 percent of the data are within the 1σ bands and 95.5 percent within the 2σ lines, the fit is assumed valid.

The confidence bands are extended beyond the range of the data at a distance ΔX_1 from the calculated line.

2. Gumbel's third asymptotic distribution

a. Order the inputs as in the double exponential distribution:

$$x_1 > x_2 > x_3 > \ldots > x_m.$$

b. Calculate the cumulative probability and reduced variate y_m for each point:

$$P(X \leq x_m) = F(x_m) = 1 - \frac{m}{M + 1}$$

$$y_m = \ln[-\ln F(x_m)].$$

c. Plot x_m versus y_m and determine approximate parameters as follows. Based on St. Denis (1975), the steps are:

(1) Draw a faired smooth curve through the maxima x_m.

(2) The initial value of the modal value μ is read from the faired curve at $y = 0$.

(3) The initial value of the upper bound $\hat{x}$ is taken as the largest value x_m in the data.

(4) The initial value of the shape factor k is obtained from

$$k = (\hat{x} - \mu)/[1/\alpha]$$

where $1/\alpha$ is the slope of the faired curve through the modal value ($y = 0$).

d. Computer search around the initial values to minimize the variance between the observed x_m and those calculated from

$$x_m = \mu + (\hat{x} - \mu) \exp(-y_m/k).$$

e. Calculate the confidence bands around the central values at a distance from the ordinate

$$\Delta X = \pm [f(p)/\alpha \sqrt{M}]n$$

where all variables are defined as for the double exponential distribution. The slope $1/\alpha$ in this calculation is a variable dependent upon y.

f. Calculate the confidence bands about the same extreme points as for the double exponential distribution. Again $1/\alpha$ is considered to be variable.

Appendix B. Analysis of Hindcast Data Specific to Keahole Point

Each of the five methods of extrapolation described in Part I were used for the analysis of the hindcast data applicable to Keahole Point. A brief description of the calculations and a summary of the results for each are presented below.

Normal distribution

The appropriate probability distribution function for the normal distribution is

$$P(H \leq h) = F(h) = 1/2 + \text{erf}\left(\frac{h - \mu_h}{\sigma_h}\right) \qquad \text{(B-1)}$$

where μ_h = the mean of the data

σ_h = the standard deviation of the data

$$\text{erf}(y) = 1/\sqrt{2\pi}\int_0^y e^{-z^2/2}\, dz.$$

The line describing the normal distribution in equation (B-1) is completely defined by the mean and standard deviation of the data. For plotting purposes each datum is assigned a probability by

$$P(H \leq h) = 1 - \frac{m}{N + 1} \qquad \text{(B-2)}$$

where m = the rank in decreasing magnitude

N = the total number of observations.

The variance of the fit is calculated by comparing the actual wave heights and those calculated from equation (B-1) at each assigned probability. Expected values of the wave height for return periods beyond the period of the record are calculated directly from the probability distribution function.

Log-normal distribution

The log-normal distribution was calculated in a manner identical to the normal distribution with the logarithm of the wave height replacing the wave height. For purposes of comparison, the variance of the fit was calculated in units of ft^2 by first converting the predicted logarithm values to actual heights. Table B-1 summarizes the intermediate calculations for the normal and log-normal distributions for the 11 storms specific to Keahole Point. The results are presented graphically in Figures B-1 and B-2.

TABLE B-1. INTERMEDIATE CALCULATIONS OF NORMAL AND ln-NORMAL DISTRIBUTIONS FOR 11 STORMS AFFECTING KEAHOLE POINT

H_a Observed Wave Height (ft)	$P(H \leq h)$ (Eq. B-2)	$\frac{h - \mu_h}{\sigma_h}$	Normal Distribution $\mu_h = 19.21$ $\sigma_h = 4.87$ H_p = Predicted Wave Height (ft)	$(H_p - H_a)^2$	ln-Normal Distribution $\mu_h = 2.92$ $\sigma_h = .065$ ln H_p	H_p	$(H_p - H_a)^2$
27.0	.917	1.383	25.9	1.12	3.276	26.5	0.29
25.5	.833	0.967	23.9	2.50	3.170	23.8	2.89
23.0	.750	0.675	22.5	0.26	3.095	22.1	0.83
22.9	.667	0.431	21.3	2.54	3.033	20.8	4.60
22.5	.583	0.210	20.2	5.14	2.977	19.6	8.29
18.9	.500	0.000	19.2	1.03	2.923	18.6	0.92
14.8	.417	-0.210	18.2	11.47	2.869	17.6	7.99
14.6	.333	-0.431	17.1	6.31	2.813	16.7	4.25
14.5	.250	-0.675	15.9	2.04	2.751	15.7	1.34
14.0	.167	-0.967	14.5	0.25	2.676	14.5	0.28
13.6	.083	-1.383	12.5	1.26	2.570	13.1	0.28
				$\Sigma = 33.91$			$\Sigma = 31.13$

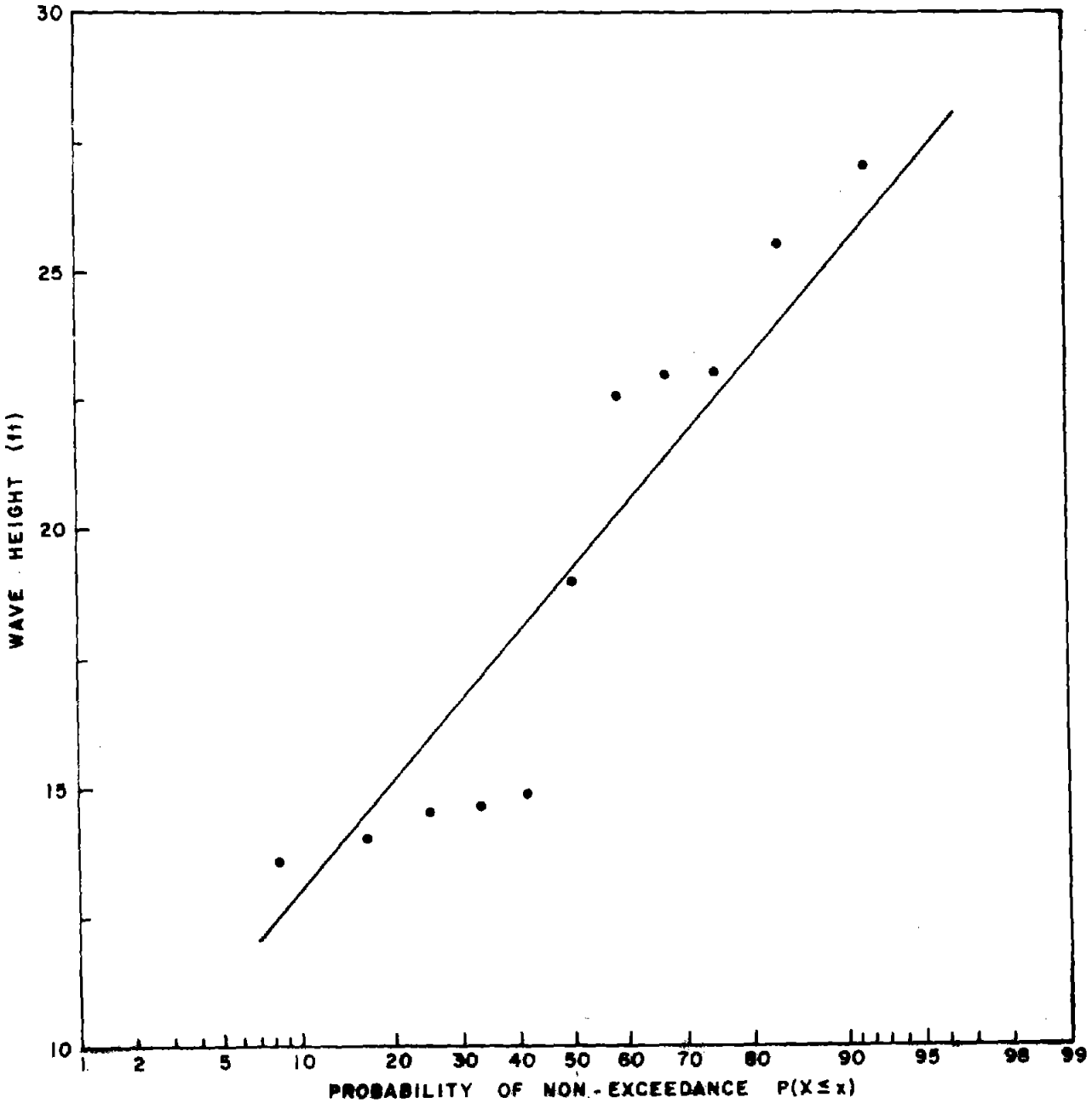

Figure B-1. Normal distribution of significant wave heights from 11 storms affecting Keahole Point

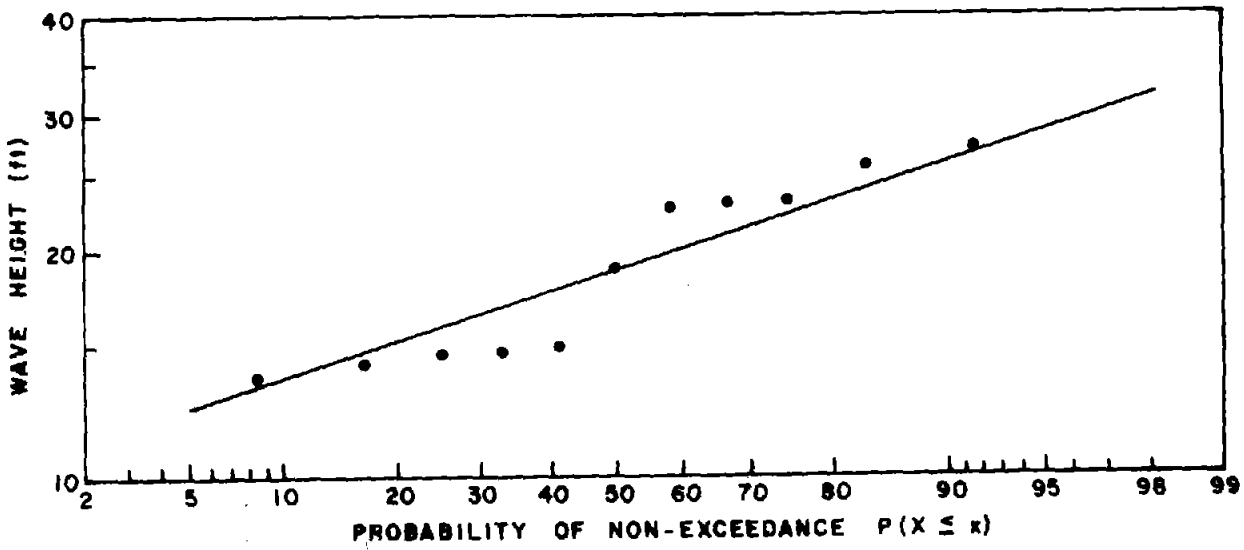

Figure B-2. Log-normal distribution of significant wave heights from 11 storms affecting Keahole Point

Semi-log plot

The coefficients for the semi-log plot were calculated using least squares, having calculated the return period from

$$T = 1/[1 - P(H \leq h)]/n \qquad \text{(B-3)}$$

where T = the return period in years

n = average number of observations per year

P = the assigned probability as calculated in equation (B-2).

For the 11 storms hindcast by the Corps of Engineers, the predicted significant wave height is given by

$$H = 9.98 + 14.75 \log_{10} T \qquad \text{(B-4)}$$

with the variance of actual to predicted values being 2.98 ft^2. These results are presented in Figure B-3.

Weibull distribution

The coefficients for the Weibull distribution were calculated with the return period adjusted to years as for the semi-log plot. To be consistent with other methods, the variance of the wave height, not the return period, was calculated. This means the ordinate and abscissa described in Part I have been reversed. Analysis for the 11 storms resulted in

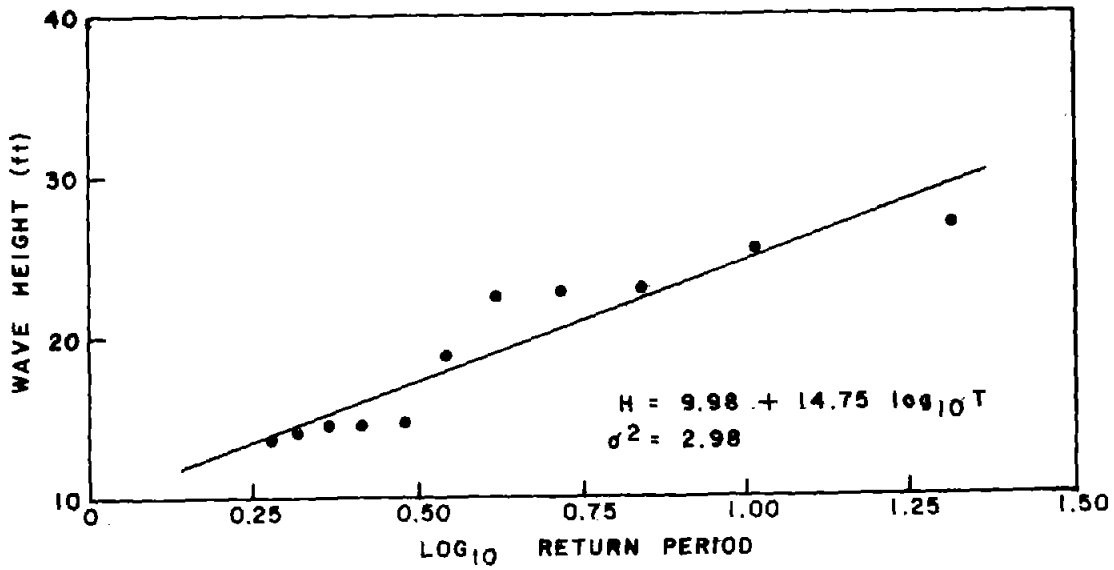

Figure B-3. Semi-log plot of significant wave heights from 11 storms affecting Keahole Point

$$\ln H = 2.79 + .515 \ln \ln T \qquad \text{(B-5)}$$

where H = the significant wave height in ft.

T = the return period in years.

These results are presented in Figure B-4. The variance of predicted to actual values is 2.11 ft^2.

Gumbel's first asymptotic distribution

The coefficients for Gumbel's first asymptotic distribution were calculated by least squares with the reduced variable defined by

$$y = -\ln\{-\ln[P(H \leq h)^n]\} \qquad \text{(B-6)}$$

where n = the average number of observations per year

$P(H \leq h)$ = the assigned probability as calculated in equation (B-2).

From the 11 storms this yields

$$H = 14.21 + 4.78\, y \qquad \text{(B-7)}$$

where the height is in feet and the variance is 1.58 ft^2.

As measured by the variance, Gumbel's first asymptotic distribution yielded the best fit. These results were presented in Figure 10. The confidence bands were calculated according to Appendix A and show the line determined to be valid for this body of data.

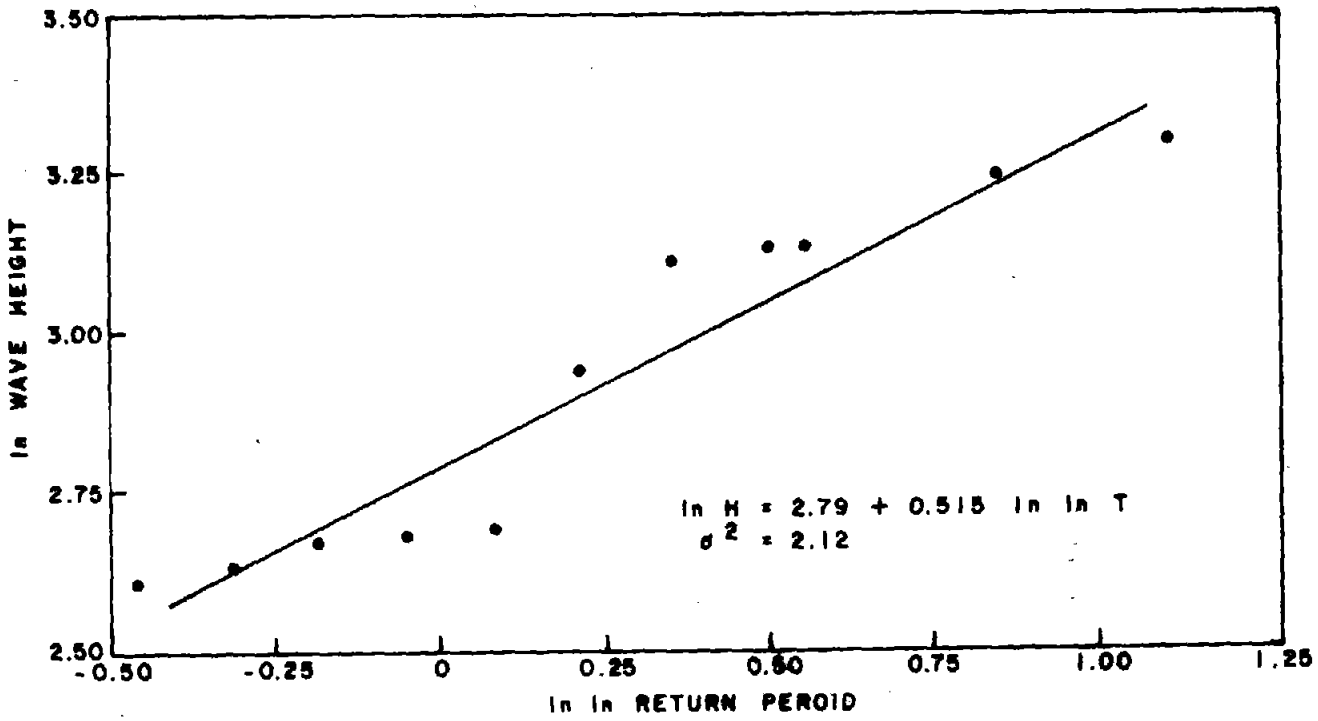

Figure B-4. Weibull distribution of significant wave heights from 11 storms affecting Keahole Point